Alma Mater Studiorum · Università di Bologna

ANALYZING BRAIN CONNECTIVITY OF DISORDER OF CONSCIOUSNESS PATIENTS WITH A MULTI-VARIATE, TIME-DEPENDENT AND ADAPTIVE ARMA MODEL

Relatore: Presentata da:
Chiar.mo Prof.   ANNA AVENA
SIMONE MARTINI

Correlatori:
Prof.ssa ANDREA FINKE
Dott. ROBERT HASCHKE

To my family and to Luca.

I love you ...

Abstract

Nell'ambito delle neuroscienze vengono effettuati sempre più studi al fine di comprendere meglio le reti cerebrali e le loro dinamiche. La comunità scientifica ha condotto numerosi studi ed esperimenti sulle normali funzioni cerebrali umane, ma solo recentemente un discreto numero di ricercatori ha rivolto la propria attenzione all'analisi di diversi disturbi cerebrali, tra cui i disturbi della coscienza (Disorders of Consciousness o DoC).

Un DoC è uno stato in cui viene meno la capacità psichica e cognitiva della persona e quest'ultima non mostra segni di veglia e/o di consapevolezza.

Questa tesi mira a sviluppare un modello che consente di analizzare la connettività neurale tra le diverse aree cerebrali e fare inferenze sullo stato dei pazienti affetti da DOC al fine di supportare e affiancare gli attuali criteri diagnostici e migliorare così il processo decisionale medico.

L'approccio utilizzato per raggiungere questo obiettivo si basa sul concetto di causalità di Granger (G-causality). Questo metodo permette l'identificazione delle interazioni causali all'interno del cervello e può essere tracciato attraverso un modello autoregressivo a media mobile (ARMA) basato sull'algoritmo delle trasformazioni di Fourier (FT).

In particolare, in questa tesi è stata implementata una peculiare normalizzazione della G-causality denominata coerenza parziale diretta (PDC). La PDC mira a stimare la connettività tra coppie di neuroni e i risultati mostrano quanto siano forti tali connessioni, permettendo così l'identificazione di pattern e la comparazione fra i diversi stati tipici dei disturbi della coscienza.

Contents

List of Figures

List of Tables

Chapter 1

Introduction

Advances in cognitive neuroscience and brain imaging technologies provides us with the ability to interface directly with the human brain.

This ability makes possible to understand brain dynamics and increase our knowledge about functional connectivity among neurons both in healthy subjects and, especially, in patients with severe brain injuries, among which disorder of consciousness (DoC) patients.

A disorder of consciousness is a state where consciousness has been affected by damage to the brain and the injured person shows no signs of wakefulness and awareness. In DoC patients the level of neuronal activity can vary depending on the state of consciousness: coma, vegetative state (VS) and minimally conscious state (MCS).

In most cases, it is difficult to distinguish among different levels of consciousness and this can lead to a misdiagnosis which impact on patients' well-being. In order to avoid that, it is important to monitor DoC patients and thanks to innovative imaging technologies such as *electroencephalogram* (EEG) systems this is made possible.

A EEG system is a suitable non-invasive technique which enables the detection and visualization of multiple activated areas in the brain so that is usually used to monitor patients.

Nevertheless, traditional diagnostic criteria are unable to infer information about patient state accurately in real-time, thus more refined diagnostic tool is necessary to improve medical decision-making.

In order to address this research question and improve and enhance existing methods, a brain connectivity analysis was developed. This allows in a online fashion, through EEG systems, to monitor patients and detect functional connectivity among several areas of the brain.

Concepts of functional brain connectivity are becoming increasingly significant in neuroscience, in this thesis a Granger causality approach was used to perform the connectivity analysis.

The advantage of using a G-causality method is that provides a powerful technique for identifying directed functional ("causal") interactions within brain and is defined in both time and frequency domains.

The GC concept can be traced in terms of a bivariate linear autoregressive-moving-average (ARMA) model and in this work, a particular normalization of the general G-causality measure named partial directed coherence (PDC) was developed.

The aim of this work is to assess instantly and continuously brain connectivity in near real time by analyzing G-causality measures using the outstanding feature of the ARMA model which allows the continuous adaptation of the model to the non-stationaries of the EEG signal.

Signals that have been analyzed derives mostly from EEG recordings that were collected from the Neuroinformatics Group of Bielefeld University in 2019. Other signals come from *Physionet.org* and were used as benchmark.

Involved tools for the preprocessing phase belongs to the library MNE - Martinos Center for Biomedical Imaging (`mne.tools/stable/index.html`).

1.1   Outline

This thesis is sectioned into the following chapters: a general description
of the most used neuroimaging techniques as well as brain connectivity foun-
dations are explained in **chapter 2**.

Chapter 3 outlines the single methods and algorithms used for comput-
ing the connectivity analysis. In particular is explained in detail the Granger
causality concept and how the ARMA model was implemented to allow brain
connectivity analysis. The materials and the methods that was specifically
used are described in **chapter 4**.

In **chapter 5** are shown the results of the computed connectivity analysis.
Finally, conclusions, improvements and future research developments are out-
lined in **chapter 6**.

Chapter 2

Background

The human brain is organized into parallel, interacting systems of anatomically connected areas and in order to understand the functions of these systems measuring connectivity is necessary [1].

Some common technologies for measuring the neural activity are functional magnetic resonance imaging (fMRI), electroencephalogram (EEG), electrocorticogram (ECoG) and multi-electrode array (MEA). Each of them is different on the basis of how much invasive is the imaging method.
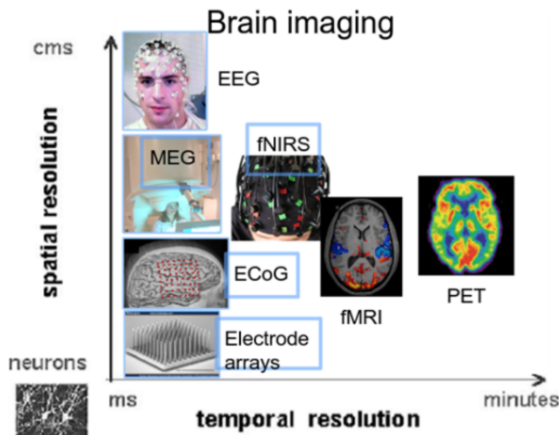
Figure 2.1: Several technologies for measuring brain activity [2].

In particular, the EEG-system is a suitable non-invasive technique which enables the detection and visualization of multiple activated areas in the brain.

In fact, it is usually used to monitor patients and diagnose several brain disorders by analyzing their brain connectivity.

In this document brain connectivity in healthy individuals and patients affected by disorders of consciousness (DoC) are analyzed.

2.1   Comparison of various neuroimaging methods

As was said before, there are several modern methods that allow neuroscientists to measure neural connectivity by using non-invasive techniques. Here a comparison of the most used in vivo imaging methods is done, with a brief description of each method, the field of application, advantages and disadvantages.

- **EEG:** *Electroencephalogram*

  EEG signal originates mainly in the cerebral cortex, a highly folded brain region in which most of information about activities (i.e. conscious awareness of sensation, body movement initiation, language and cognitive functions) takes place.

  Brain activity is measured by unpolarized electrodes placed at scalp level. Generally EEG signals belong to a frequency band between 0 and 50 Hz with a rather high time resolution.

  In contrast, the physical localization of the source signal is inaccurate.

- **fMRI:** *Functional magnetic resonance imaging*

  fMRI is a technique which measures brain activity by scanning repeatedly brain volume using a MRI tomography. It is denoted as a BOLD (Blood Oxygenation Level Dependent) signal and its 3D results have

an excellent spatial resolution while its temporal resolution is dramatically worse than for EEG because the period of each scan is in the order of seconds.

- **NIRS:** *Near infrared spectroscopy*

  NIRS is a optical imaging technique based on low level of light that, passing through living tissue, can measure oxygenation by the functional state of the tissue.
  NIRS signal is based on capillary-oxygenation-level-dependent (COLD) signal.
  This technique is able to find hemodynamic changes associated with the brain activity.

- **MEG:** *Magnetoencephalogram*

  MEG measures the magnetic fields generated by neuronal activity of the brain.
  It records the magnetic flux from neurons' synaptic discharge, and these measurements are done in magnetically shielded rooms, using sensitive superconducting quantum interference devices (SQUIDS).
  SQUID amplifies the weak extra cranial magnetic field and converts it into a voltage, then .
  MEG data shares the basic features and frequency content of EEG, with predominant activity in delta band, frequency less than 4 Hz

Generally each modality is analyzed separately, e.g. when is considered electrophysiological response, hemodynamic response or brain activity separately. However, for a better understanding of connectivity, it is possible to combine more methods together. Hence, four multimodal paradigms are developed:

1. EEG and MEG: electrical signals measured from the surface of the head are strictly correlated with the magnetic field generated by the motor cortex. Thus, this approach, also called EMEG, can add additional

information to single modality EEG or MEG with regard to source reconstruction of brain activity, in particular covers all localizations and the improved result is due to the different properties of the two imaging modalities rather than simply due to increased total channel number.

2. EEG and fMRI: this concurrent modality research provides excellent temporal resolution (in order of milliseconds) given by EEG recordings while fMRI gives a high spatial resolution. This paradigm provides new possibilities in the investigation of brain rhythms, sleep patterns and epilepsy due to the integration of these two technologies in a hybrid solution, allowing simultaneous acquisition of the two signals by the novel EEG-fMRI technology [36].

3. NIRS and EEG: this measurement depends on several physical properties such as conductivity, absorption and scattering coefficients of the head tissues and cerebral blood flow.
   This concurrent modality finds its application in many fields thanks to its simple and comparatively low-cost setup.
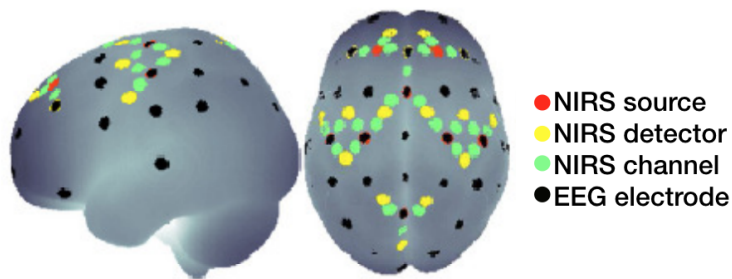
Figure 2.2: Locations of EEG electrodes and source, detectors and channels of NIRS System [35].

4. fMRI and NIRS: are higly correlated since neuronal activity influences both BOLD signal in fMRI image and COLD in NIRS signal. This concurrent paradigm offers a better understanding of brain activation with regard to cognitive and behavioral changes. In figure 1.3 is shown the chain of events and factors that links fMRI and NIRS.
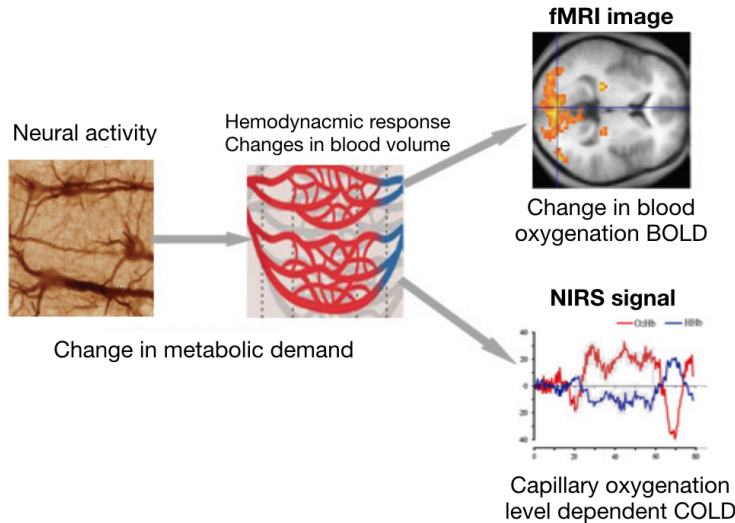
Figure 2.3: Neuronal correlates of BOLD and COLD signal [37].

In table 1.1 are summarized most relevant non-invasive imaging modalities.

Imaging method	Resolution	Application	Advantages	Disadvantages
EEG	S-low T-high	Study various rhythms, epilepsy, preoperative mapping, degenerative disorders	Non-invasive, no ionizing radiation, widely used, low cost	Low spatial resolution
fMRI	S-medium T-high	Study epilepsy	Non-invasive, no ionizing radiation, can identify epileptic foci	Low spatial resolution
NIRS	S-high T-low	Preoperative mapping, functional mapping	Non-invasive, can perform functional imaging	High cost
MEG	S-low T-high	Functional mapping	Non-invasive, low cost, no ionizing radiation	Low spatial resolution

Table 2.1: S: spatial resolution; T: temporal resolution.
Overview of neuroimaging non-invasive techniques [34].

2.2 Brain connectivity

In analysis of brain connectivity, three types of connectivity are used to describe interactions of neural networks: structural, functional and effective connections.

Structural connectivity or anatomic connectivity represents the phisical connectivity between brain regions. It is difficult to directly assess anatomical connectivity in humans, in fact this can be done only post-mortem. Many scientific studies show that the *structural connectoma* remains relatively stable in healthy adults while alterations can occur by aging or disease [13, 14];

Functional connectivity exists between regions that do not display direct anatomic connectivity [3] thus it is related to similar patterns of activation in different brain regions when a variety of different tasks are done. Functional connectivity is usually measured during resting state fMRI and is typically analyzed in terms of correlation, coherence and spatial grouping based on temporal similarities [4];

Effective connectivity is defined as the direct influence of one brain region on the physiological activity recorded in other brain regions [5] this claims to make statements about causal effects among tasks and regions.

In the present work, the attention is focused on functional association between neurons, because is more interesting to obtain the functional connectivity (FC) between brain regions, and not the structural one, even if when computed over long sessions at rest, the whole brain map of functional connections, generally termed *functional connectome*, reveals some similarities with the structural connectome [12].

Assuming a stationary perspective, there are several methods for analyzing FC and detect networks of brain areas showing coherent increases and

decreases of activity, the most common methods are:

- **Seed-based connectivity analysis** is the oldest method, it consists of extracting the average blood oxygenation level dependent (BOLD) time course from a region of interest (seed region) and then determining the temporal correlation between this extracted signal and the time course from all other brain voxels. The main disadvantage is that its results depend on the a priori definition of a seed region, however, it may be particularly useful if the interest is in investigating connections with specific areas of the brain.

- **Hierarchical clustering** requires a priori definition of seed regions but instead of extracting time course from just one (or few) seed region, time courses are extracted from many brain areas and then a correlation matrix is constructed. A clustering algorithm may be used to determine which regions are more distantly related and also hierarchical trees or topological maps can be constructed to represent global and local properties of brain networks [15].

- **Indipendent component analysis** (ICA) has become one of the most common methods of network generation in steady state functional connectivity. ICA divides fMRI signal into several spatial components that are maximally independent in a statistical sense. Each component is associated with a spatial map, some maps corresponding to noise components, others to neuro-anatomical systems. This method is data-driven and automatically isolates sources of noise, but it is highly dependent on the number of components.

In the table below are summarized the advantages of these methods of analysis:

However, recent studies suggest that spatial patterns of a resonance imaging network may change periodically over the time of an fMRI acquisition.

Method	Benefits and advantages
Seed based connectivity	- Inherent simplicity; - good sensitivity; - easy to be interpreted.
Hierarchical clustering	- Allows abstract properties of complex systems to be quantitatively characterized and mapped; - captures global tendencies and local topological properties.
Indipendent component analysis	Determine the underlying structure of data that often is difficult to specify a priori.

Table 2.2: Methods for analyzing functional connectivity

For this reason, a dynamic functional connectivity (DFC) analysis has been implemented. Thus, for analyzing DFC, are performed:

- **Sliding window analysis** which is the method most used in the analysis of functional connectivity. This analysis is performed by conducting analysis on a set number of scans in an fMRI session and the number of scans represents the length of the sliding window. The defined window is then moved a certain number of scans forward in time and additional analysis is performed. The movement of the window is usually referenced in terms of the degree of overlap between adjacent windows. As the most common method of analysis, sliding window analysis has been used in many different ways to investigate a variety of different characteristics and implications of dynamic functional connectivity (DFC). In order to be accurately interpreted, data from sliding window analysis generally must be compared between two different groups. Researchers have used this type of analysis to show different DFC characteristics in diseased and healthy patients, high and low performers on cognitive tasks and between large scale brain states.

- **Activation pattern analysis** is one of the first methods ever used to analyze functional connectivity of fMRI images to show that there are patterns of activation in spatially separated brain regions that tend to have synchronous activity. It has become clear that there is a spatial and temporal periodicity in the brain that probably reflects some of the constant processes of the brain. Repeating patterns of network information have been suggested to account for $25-50\%$ of the variance in fMRI BOLD data [6, 7]. These patterns of activity have primarily been seen in rats as a propagating wave of synchronized activity along the cortex. These waves have also been shown to be related to underlying neural activity and has been shown to be present in humans as well as rats.

- **Point processing analysis** is departing from the traditional approaches, in fact this method transforms the fMRI BOLD data into a point process [8]. This is achieved by selecting for each voxel the points of inflection of the BOLD signal (i.e., the peaks). These few points contain a great portion of the information pertaining functional connectivity, because it has been demonstrated, that despite the tremendous reduction on the data size ($> 95\%$), it compares very well with inferences of functional connectivity obtained with standard methods which uses the full signal [9].

- **Other methods** like time-frequency analysis has been proposed as an analysis method that is capable of overcoming many of the challenges associated with sliding windows. Unlike sliding window analysis, time frequency analysis allows the researcher to investigate both frequency and amplitude information simultaneously. The wavelet transform has been used to conduct functional connectivity analysis that has vali-

dated the existence of afunctional connectivity by showing its significant changes in time.

In the table below are summarized the advantages of these methods of analysis:

Method	Benefits and advantages
Sliding window	- Any steady state analysis can be performed using sliding window if the window length is sufficiently large; - it is easy to understand and in some ways easier to interpret [3].
Activation patterns	High stability and separation ability
Point process analysis	- Clarification of what the response variable is that is modelled; - ways forward regarding difficult issues for sampling bias [11].
Time-frequency analysis	- Has broad scope of applications; - enables one to talk sensibly about signals whose component frequencies vary in time

Table 2.3: Methods for analyzing dynamic functional connectivity

2.3 Disorders of consciousness and brain functional connectivity

Most of the brain energy consumption is related to intrinsic activity that is not driven by responses to external stimuli [10]. Energy associated with evoked brain activity accounts for less than 5% of the total brain energy budget thus resting state fMRI technique enables the study of brain functioning both in healthy subjects and in patients with disorders of consciousness, because these are not required to perform any task.

In particular, in disorder of consciousness (DoC) it is possible to distinguish among different levels of consciousness, from totally unconscious to totally conscious.

Usually two dimensions of consciousness are taken into account for describing the different DoC states: wakefulness and awareness. The first one refers to the ability to directly know and perceive, to feel, or to be cognizant of events; the latter represents a state of consciousness in which an individual is conscious and engages in coherent cognitive and behavioral responses to the external world.
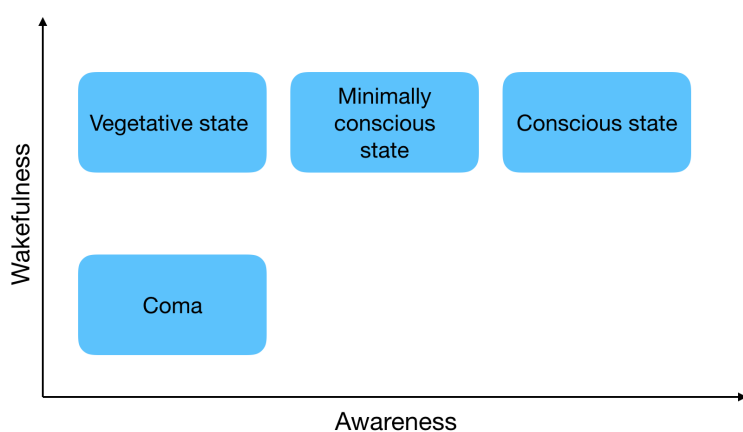
Figure 2.4: States of consciousness.

Several categories of disorders of consciousness can be distinguished on the basis of these two dimensions [16, 17]. Coma is characterised by complete absence of both signs of wakefulness and awareness. A state of wakefulness without awareness is called a vegetative state (VS) or more recently unresponsive wakefulness syndrome [18]. A minimally conscious state (MCS) refers to a state of wakefulness with only minimal signs of awareness.

Diagnosis of disorders of consciousness is commonly based on a scale which evaluates and differentiate levels of consciousness, the Glasgow coma scale (GCS) is usually used for initial assessment of a person's level of consciousness after a head injury.
GCS scale is composed of three tests: eye, verbal and motor responses. The three values separately as well as their sum are considered. The lowest possible GCS (graded 1 in each element) is 3 (deep coma or death), while the highest is 15 (fully awake person).

	1	2	3	4	5	6
Eye	Does not open eyes	Open eyes in response to pain	Opens eyes in response to voice	Opens eyes spontaneously	-	-
Verbal	Makes no sounds	Makes sounds	Words	Confused, disoriented	Oriented, converses normally	-
Motor	Makes no movements	Extension to painful stimuli	Abnormal flexion to painful stimuli	Flexion / Withdrawal to painful stimuli	Localizes to painful stimuli	Obeys commands

Figure 2.5: Glasgow coma scale [19].

Generally, brain injury is classified as:

- Severe, GCS $< 8-9$

- Moderate, $9 \leqslant$ GCS $\leqslant 12$

- Minor, GCS $\geqslant 13$

Other scales which provide more detailed assessments of consciousness are Wessex Head Injury Matrix (WHIM) or JFK Coma Recovery Scale - Revised version (CRS-R). However, signs of consciousness depend on the patient's level of arousal, which can be fluctuating. Furthermore assessment of consciousness can be complicated by other factors: motor impairment, tracheotomy or habituation to stimuli [20]. These and other factors can lead to a misdiagnosis in patients with DoC, in fact as many as 40% of patients with a diagnosis of vegetative state may retain some level of consciousness [21].
An additional difficulty is the distinction between disorders of consciousness and the locked-in syndrome. Patients with locked-in syndrome are both awake and aware, yet they are entirely unable to produce any motor output or they have an extremely limited repertoire of behaviours (usually vertical eye movement or blinking).
If motor functions have been lost completely, current behavioural diagnostics can not distinguish between the locked-in and the vegetative state. Neuroimaging methods, like EEG, provide a tool to assess overall electrical signal content for detecting the level of awareness and potentially aid the prediction of the chance of recovery a patient [16].
With EEG it is also possible to monitor the ability of a person to process external stimuli through the event related potentials (ERP). However, other imaging methods are considered more accurate for the localization of the source signal, namely emission tomography (PET) and magnetic resonance imaging (MRI).

Some recent studies show the correlation between consciousness and auditory function, in particular has been discovered that theses auditory paradigms not only assess consciousness, but also sensory function.
The presence of primary auditory cortex activation is not in itself evidence for consciousness. In fact a study of propofol induced anaesthesia showed that primary auditory cortex activation is still present even in deep sedation [22]. It is thus necessary to assess higher order function to obtain results about the

level of consciousness. The higher-order processing can be assessed through the speech paradigm or the imagery paradigm. This latter provides that the subject imagine to do a specific task like moving around ones own house (spatial navigation task), imagining singing a song, imagining playing tennis and imagining faces. The imagination of moving around ones own house and of playing tennis showed the most robust results. These two tasks were also used in a case study of a patient diagnosed with VS. This patient did not only show intact auditory function, evidenced by a prior test of speech processing, but could also distinctly perform both imagination tasks [23]. Further research showed that some patients were able to answer yes/no questions using a imagination paradigm, this result shows that mental imagery is a powerful tool to identify patients that seem to be unaware behaviourally, but are in fact only impaired in their ability to perform the behavioural tasks [38].

2.4 EEG-System

Electroencephalography is a completely non-invasive electrobiological measurement that reads scalp electrical potentials generated by brain dynamics.
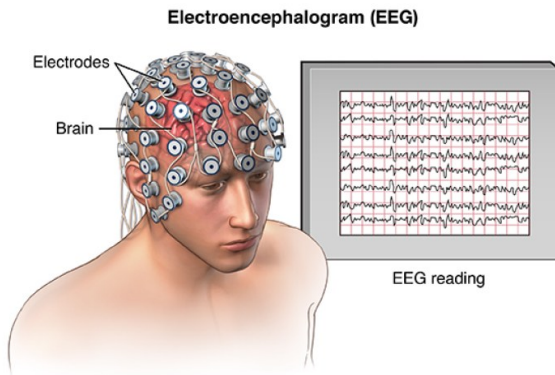
Figure 2.6: EEG system [25].

The electroencephalogram (EEG) is defined as electrical activity of an alternating type recorded from the head surface after being picked up by metal electrodes and conductive media [24]. The first account, by Richard Caton, documenting the recording of spontaneous brain electrical activity from the cerebral cortex of an experimental animal dates back to 1875. Next to Caton, Hans Berger, introduced the electrical brain recording method to humans in 1924. This method was able to measure the irregular, relatively small electrical potentials generated in the brain without opening the skull.

2.4.1   EEG measurement

EEG measures variations in electrical field generated by groups of neurons in the brain cortex: when neurons are activated, local current flows are produced [26]. Neurons' activation is also called *action potential*: it represents a short lasting event in which the electrical membrane potential of a cell rapidly rises and falls. After an action potential has occurred, there is a transient negative shift called the *refractory period*. Neurons use this mechanism to prevent firing another action potential immediately.
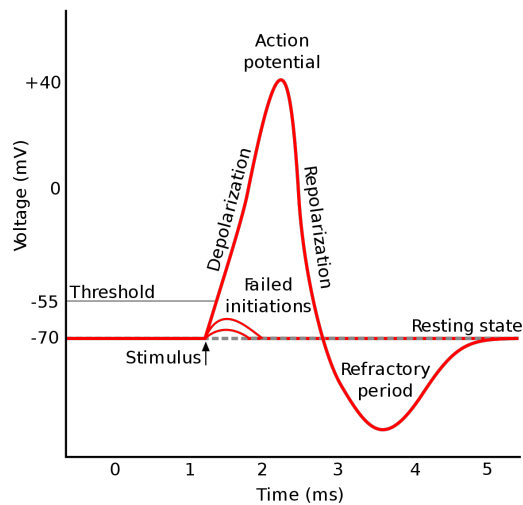
Figure 2.7: View of an action potential and its various phases.

The simultaneous activation of various neurons produces current fluxes, and hence electrical fields, that can sum up and hence can be registered with electrodes positioned on the scalp.
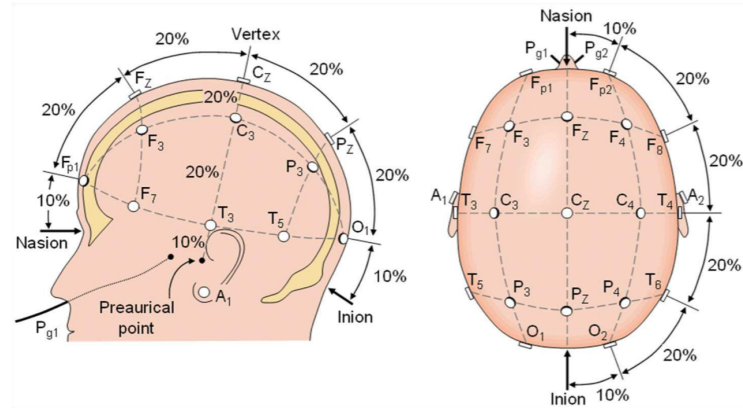
Figure 2.8: EEG electrode setup internationally standardized 10-20 system [25]. Electrode placements are labelled according adjacent brain areas: F (frontal), C (central), T (temporal), P (parietal), and O (occipital).

The electrical contribution of each neuron is extremely small and the signal must pass through various layer of non-neuronal tissue before reaching the electrodes. Therefore, thousands of neurons activated simultaneously are necessary to generate a signal that can be measured with EEG. The amplitude of the EEG signal depends strongly on how the activity of involved neurons is synchronized. Typically the amplitude of the electrical potentials measured on the scalp varies between 20 and 100μV and the oscillations have frequencies between 1 and 60Hz [38].
These frequencies are usually classified in the following frequency bands:

delta $[< 4$ Hz$]$: deep sleep, unconsciousness, coma.

theta $[4 - 7$ Hz$]$: in sleep stages, meditation, short-term memory.

alpha $[8 - 12$ Hz$]$: relaxation, tiredness, eyes closed (but awake).

beta $[13 - 30 \text{ Hz}]$: awake, focused, active.

gamma $[> 30 \text{ Hz}]$: conscious waking state, memory.
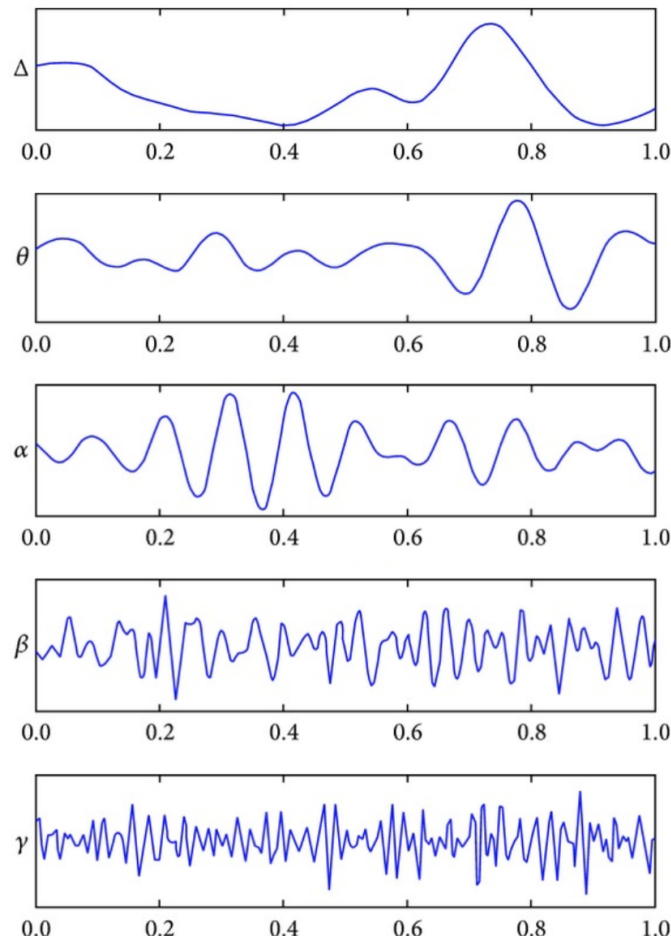
Figure 2.9: Cerebral spontaneous activity.

The analysis of cerebral spontaneous activity reveals different mental states (such as concentration or relaxation), different conscious states (e.g. sleep or awake) or some pathologic disturbs.

2.4.2 EEG analysis pipeline
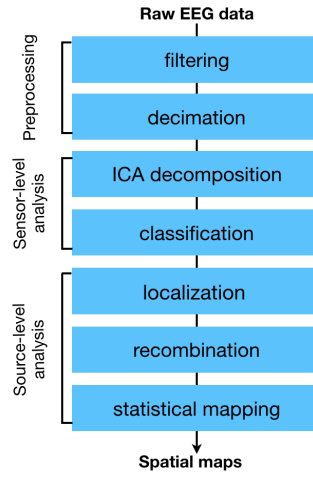
Figure 2.10: EEG pipeline.

Spontaneous activity constitute a large and complex amount of data, this is the reason why EEG data needs to be preprocessed. Furthermore, EEG preprocessing pipeline can reduce the signal-to-noise ratio [27]. This process consists of several phases:

- **Band-pass filter** (BPF) apply a high-pass filter to filter out slow frequencies less than 0.1 Hz or often even 1 Hz and a low-pass filter to filter out frequencies above 40 or 50 Hz. This filtering process is done for allowing to focus only on frequencies that are interesting to analyze.

- **Decimation** (also known as *downsampling)* decrease sample rate of a sequence to a lower rate. In figure 1.11 is shown this process.

- **ICA decomposition** (or any linear decomposition method, including PCA and its derivatives) is a computational method for separating a multivariate signal into additive subcomponents. This is done by assuming that the subcomponents are non-Gaussian signals and that they are statistically independent one from each other.
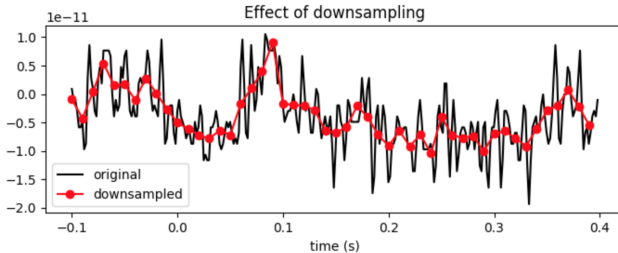
Figure 2.11: Downsampling from 600 Hz to 100 Hz.

- **Classification** approach for EEG data has been changed in last decade. Originally were explored five main families of classifiers: linear classifiers, neural networks, non-linear Bayesian classifiers, nearest neighbour classifiers and classifier combinations.
  Nowadays many new algorithms have been developed and tested to classify EEG signals, these can be divided into four main categories: adaptive classifiers, matrix and tensor classifiers, transfer learning and deep learning. Among these, adaptive classifiers were demonstrated to be generally superior to the static one [28].

- **Localization** is used to localize the electrical activity of brain, it provides useful information for the study of brain's physiological, mental and functional abnormalities. The electrode locations are often available with the acquisition systems.

- **Recombination** represents a technique used for the reconstruction of the brain activity in the source space after having performed the ICA decomposition and the classification. Furthermore, some studies show that the recombination approach is more effective when applied after source localization [29].

- **Statistical mapping** refers to the construction and assessment of spatially extended statistical processes used to test hypotheses about functional imaging data.

2.5 Brain-Computer Interfaces

Brain Computer Interfaces (also called *Brain Machine Interfaces*, BCIs/BMIs) use neural information derived from brain activity to control external devices. The development of BCI systems is mainly focused on improving functional independence for individuals with severe motor problems. The development of neural interfaces not only has clinical implications but is also a powerful tool in the hands of neuroscientists: the main challenge is coding and decoding brain activity and make possible the direct communication in real time between the subject and the external device.
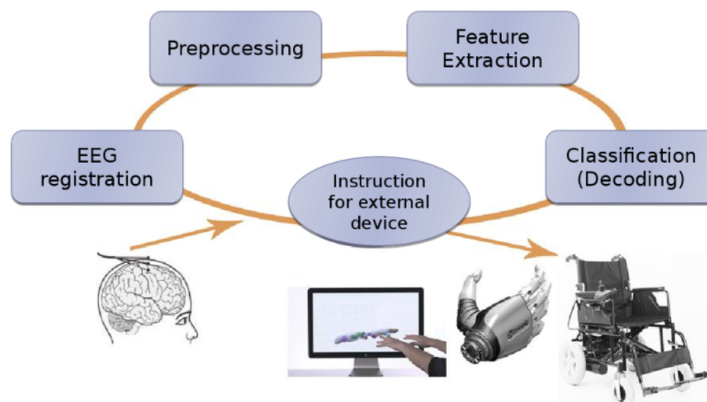
Figure 2.12: Phases of BCI decoding.

Although there are many types of BCIs, there are key components common to all of them:

1. the recording system that extracts neural activity;

2. the decoding system that translates this data into action signals;

3. the actuator system controlled by the generated signals.

These points define a typical open-loop neural interface.
What distinguishes an open-loop interface from a closed-loop interface is that

a sensory feedback is added to the closed-loop interface: it can be represented by the simple observation of the actuator movement (mechanical prosthesis, movement of a cursor on a screen, etc.). The goal of a neural interface is to allow an individual to communicate with the world outside, using only the cerebral signals emitted by the brain.

Chapter 3

Connectivity analysis

EEG traces are time series of electrical potential fluctuations recorded at various scalp locations that reflect the physiological behavior of the underlying brain cells [30].

Spontaneous EEG signals, after being recorded, can be analyzed in time-domain or in frequency-domain. While time-domain analysis shows how a signal changes over time, frequency-domain analysis shows how the energy of the signal is distributed over a range of frequencies. Both methods have advantages (+) and drawbacks (-) as shown in the following table:

Frequency-domain	Time-domain
+ More flexibility	+ Filtering consists of sums and products
+ Short-time analysis works with consecutive, possibly overlapping, signal segments	+ Filtered series can be immediately plotted
- Analysis precision is limited by the windowing operation and non-stationarity	- Requires the application of two Fourier transforms, this can lead to computational errors

Table 3.1: Advantages and drawbacks of frequency-domain and time-domain.

A signal can be converted between time and frequency domains with a pair of mathematical operators called *transform*.

Regarding EEG signals, the most commonly used is the Fourier Transform (FT), which decomposes a function into the sum of a (potentially infinite) number of sine wave frequency components. The result is represented in a spectrogram or a power spectrum. The latter presents the amplitude and the frequency content of a signal in a particular point of time. A spectrogram differs from it because contains also information about how amplitude and frequency differs over time and basically is the result of a series of Fourier transformations applied sequentially to a signal.

Power spectra and spectrograms do not contain phase information.
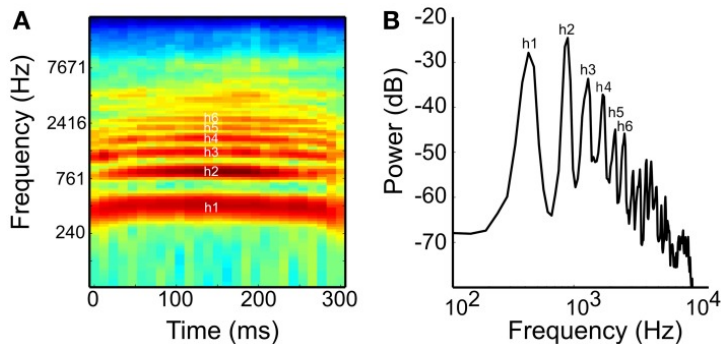
Figure 3.1: Example of a generic (A) spectrogram and (B) power spectrum.

In this thesis, brain connectivity was analyzed in frequency domain and the used approach is based on an autoregressive moving-average model which rely on a Granger causality concept.

In the following paragraphs are described both the general idea and more in detail the process behind those notions, with reference to the implementation aspect of this model.

3.1   Granger causality

This method is aimed to estimate the directionality or the causality (or causal interactions) between two signals.

The Granger causality test is a statistical assumption test for estimating whether one signal is useful for detecting another.

A signal or more generally a time series X is said to Granger-cause Y if it can be shown that those X values give a statistically remarkable information about the evolution of the values of Y or vice-versa.
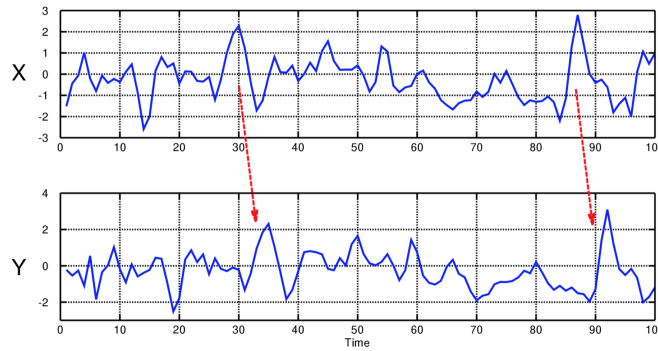
Figure 3.2: When time series X Granger-causes time series Y, the patterns in X are approximately repeated in Y after some time lag (two examples are indicated with arrows). Thus, past values of X can be used for the prediction of future values of Y [33].

The general method to estimate the values of Granger causality needs the requirement of stationarity of the signals. Therefore, due to the non-stationarity of brain signals, there is no possibilities for transient pathways of information transfer to be known. Thus, the main issue of applying time-variant Granger causality to biological signals is the declaration of adjustable thresholds for coupling EEG signals and also for the directions of causal interactions [32]. However, is possible detecting interactions with superior direction between two EEG signals for very short-lasting time intervals.

In neuroscience, Granger causality analysis is usually performed by fitting a

vector autoregressive model to the EEG traces. In this study an autoregressive moving-average (ARMA) model was carried out.

3.2 ARMA model

Adaptive classifiers are models whose parameters are incrementally re-estimated and updated over time as new EEG data become available. The adaptive model that was used in this work is a bivariate autoregressive-moving-average ARMA(p,q) model in which q is the order of the moving average and p is the order of the autoregression.

This model consists of two parts, an autoregressive (AR) part and a moving average (MA) part. The AR part involves regressing the variable on its own past values. The MA part involves modeling the error term as a linear combination of error terms occurring contemporaneously and at various times in the past.
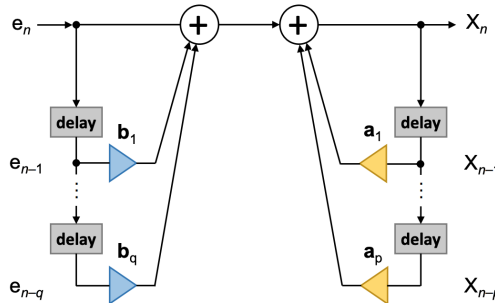
Figure 3.3: Graphical representation of ARMA model [40].

For the autoregressive part the A matrix is defined as follows:

$$A_k(n) = A_k(n-1) + c_n e_n * x_{n-k}^T \quad for \quad n > k, k = 1, ..., p \qquad (3.1)$$

For the moving-average part the matrix B is defined as:

$$B_j(n) = B_j(n-1) + c_n e_n * e_{n-j}^T \quad for \quad n > j, j = 1, ..., q \qquad (3.2)$$

The sequence c is the adaption factor for calculating new parameters and is generated by:

$$c(n) = \frac{f}{1 + (\sigma_{x1}^2(n) + \sigma_{x2}^2(n))} \qquad (3.3)$$

where f is a positive constant factor and σ are estimations of the momentary variances of the time series at time point n defined as:

$$\sigma_{x_i}^2(0) = 0$$

$$\sigma_{x_i}^2(n) = \sigma_{x_i}^2(n-1) - c_s(\sigma_{x_i}^2(n-1) - (x_n * i)^2)$$

$$for \quad n = 1, 2, ...; i = 1, 2$$

The vector e represents the sequence of errors and it is calculated as follows:

$$e_0 = 0$$

$$e_n = x_n - \sum_{k=1}^{p} A_k(n-1)x_{p-k}^T - \sum_{j=1}^{q} B_j(n-1)e_{q-j}^T$$

$$for \quad n > 0 \qquad (3.4)$$

Now the transfer function $H_n(\lambda)$ can be calculated as follows:

$$H_n(\lambda) = A_n^{-1}(\lambda) * B_n(\lambda) \qquad (3.5)$$

with

$$A_n(\lambda) = I + \sum_{k=1}^{p} A^k(n)e^{-ik\lambda} \qquad (3.6)$$

and

$$B_n(\lambda) = I - \sum_{j=1}^{q} B^j(n)e^{-ij\lambda} \qquad (3.7)$$

Coefficients in equation (2.6) and (2.7) are derived by applying the Fourier transforms (FT). See section 2.2.3 for more details.

At this point it's possible to estimate the spectral density matrix which is represented as:

$$f_n(\lambda) = h_n(\lambda) * S_n * H_n^T(\lambda) \quad for \quad n = 0, 1, 2, \ldots \tag{3.8}$$

and S_n represents the covariance matrix of prediction errors:

$$S_n = \begin{pmatrix} S_{11}(n) & S_{12}(n) \\ S_{21}(n) & S_{22}(n) \end{pmatrix}$$

with

$$S_{ij}(0) = 0 \quad for \quad i, j = 1, 2$$

$$S_{ij}(n) = s_{ij}(n-1) - c_s(s_{ij}(n-1) - e_i(n) * e_j(n))$$

$$for \quad n = 1, 2, \ldots and \, i, j = 1, 2 \tag{3.9}$$

So far it is possible to obtain a very fast estimation procedure for describing changes in the dependence of two signals.

3.2.1 Partial directed coherence

A Partial Directed Coherence (PDC) analysis can be done by performing:

$$PDC_{ij}(f) = \frac{H_{ij}^{-1}(f)}{\sqrt{h_j^{-1}(f) * h_i^{-1}(f)}}$$

Now it is possible to resolve the existence of direct connections between pairs of structures which is a concept that relies on a frequency domain representation of Granger's causality.

In particular, PDC estimator, characterizes the outflow from channel j to channel i at frequency f.

3.2.2 Directed transfer function

The Directed Transfer Function (DTF) analysis is normalized with respect to the structure that receives the signal.

The function is defined as:

$$DTF_{ij}(f) = \frac{H_{ij}(f)}{\sqrt{h_j(f) * h_i(f)}}$$

In this case the DTF estimator describes the causal influence of channel j on channel i at frequency f.

3.2.3 Fourier transform analysis

This analysis is usually done thanks to the characteristic of EEG signal which can be represented both in time and frequency domain. Fourier transform analysis, in fact, can describe frequency and also spectral content of the signal at each time point.

Hence, given a EEG signal represented in time domain, by applying the Fourier transform it is possible to represent this time domain into a frequency domain:

$$X(f) = A^{-1}(f)\epsilon(f) = H(f)\epsilon(f)$$

where $H(f)$ is the transfer function and $A(f)$ is the Fourier transform of the coefficients.

Advantages

The main advantage of Fourier analysis is that, during the transformation, only little information is lost from the signal. In fact, Fourier transform maintains information on amplitude, harmonics, and phase and uses all parts of the waveform to translate the signal into the frequency domain.

The preservation of phase information makes possible the signal to be transformed back into the time domain [31].

Disadvantages

The major disadvantage of the Fourier transformation is the inherent compromise that exists between frequency and time resolution.

The length of Fourier transformation used can be critical, it may be that no single length of transform is ideal for a particular signal; several transformations, each of a different length, may be required before a signal can be described adequately [31].

Chapter 4

Material and methods

In this chapter are briefly described participants of data recordings and datasets structure as well as the quality and technical specifications of EEG recordings. The goal is to analyze DoC patient's data which has no labels, making possible a comparison with a control group of healthy subjects, and finding patterns between sleep recordings in the control group and in patients affected by consciousness disorders. What I have done to reach this objective is to preprocess data in order to allow a comparison between the different datasets and then carry out a connectivity analysis and highlight brain dynamics that occurs in both DoC and healthy individuals.

4.1   Participants

Various individuals were involved in this work, they can be divided into 2 groups:

1. **DoC patients:** 16 subjects in comatose state.
   The age ranges from 22 to 67 years, with an average age of 44.3.
   Recordings were made on 7 female and 9 male patients in coma since an average time of 8.0 years (which ranges from 2 to 17 years).
   All the recording sessions were kept in June, July 2017.

2. Other subjects, among which:

   - **3 Healthy subjects:**

ID N.	Gender	Age	Recording date
Hs - I	Male	34	01/01/2009
Hs - II	Female	28	01/01/2007
Hs - III	Male	29	01/01/2003

   - **A insomnia patient:** female, 47 years old, recorded on 01/01/2011.

   - **A REM behavior disorder patient:** male, 58 years old, recorded on 01/01/2007.

   - **A sleep-disordered breathing patient:** male, 65 years old, recorded on 01/01/2010.

4.2   Data acquisition

- **DoC patients**
  Recordings were collected from the Neuroinformatics Group of Bielefeld University in 2019. The EEG-system that was used is a 32 channels cap with electrodes positioned according to the international 10-20 system. The sampling rate is about 2048 Hz (for facilitate computational calculus data was downsampled by factor 20 for a final sampling rate of 102,4 Hz).
  The duration of recordings is about ~ 78 minutes.

- **Other subjects**
  Recordings derive from *Physionet.org* [41] which is a repository of freely-available medical research data Sleep Database, managed by members of the MIT Laboratory for Computational Physiology.
  The sampling rate vary from 256 to 2048 Hz (again, for computational reasons were all downsampled to 102,4 Hz).

4.3   Datasets

The DoC dataset was previously high-pass filtered using 0.1 Hz cutoff, then data was downsampled (from 2048 Hz to 102.4 Hz) using the resample function from mne toolbox [42] and afterwards data was cleaned using Artifact Subspace Reconstruction (ASR). All these preprocessing steps are described in section 3.4. Regarding the other datasets, no preprocessing step was performed, except for the downsampling, because data was previously filtered and cleaned.

Recordings are available in a European Data format (EDF) which allows the exchange and the storage of multichannel biological and physical signals.

It became de-facto the standard for EEG recordings in neuroscience research projects. Information about each sleep recording can be easily obtained and an example is shown below:

```
<Info | 16 non-empty fields
    bads : list | 0 items
    ch_names : list | Fp2-F4, F4-C4, C4-P4, P4-O2, F8-T4, T4-T6, FP1-F3, ...
    chs : list | 22 items (EEG: 21, STIM: 1)
    comps : list | 0 items
    custom_ref_applied : bool | False
    dev_head_t : Transform | 3 items
    events : list | 0 items
    highpass : float | 0.0 Hz
    hpi_meas : list | 0 items
    hpi_results : list | 0 items
    lowpass : float | 256.0 Hz
    meas_date : tuple | 2007-01-01 22:36:46 GMT
    nchan : int | 22
    proc_history : list | 0 items
    projs : list | 0 items
    sfreq : float | 512.0 Hz
    acq_pars : NoneType
    acq_stim : NoneType
    ctf_head_t : NoneType
    description : NoneType
    dev_ctf_t : NoneType
    dig : NoneType
    experimenter : NoneType
    file_id : NoneType
    gantry_angle : NoneType
    hpi_subsystem : NoneType
    kit_system_id : NoneType
    line_freq : NoneType
    meas_id : NoneType
    proj_id : NoneType
    proj_name : NoneType
    subject_info : NoneType
    xplotter_layout : NoneType
>
```

Figure 4.1: Information content of a generic EDF data set.

4.4 Preprocessing

For the preprocessing phase, a powerful *Python* tool was employed: Martinos MNE [42] library. This open-source Python software allows to easily preprocess and prepare EEG (and MEG) data for further analysis.

For the connectivity analysis carried out in this work, each preprocessing phase is described more in detail below.

4.4.1 Band-pass filtering

This is a common preprocessing step for connectivity analysis because most relevant frequencies usually lie between 1 and 30 Hz. In particular, slow signal fluctuations above 1 Hz are considered noise for this type of analysis.

It is important to apply a band-pass filter for both healthy subjects and DoC patients because neural activity overlaps entirely with muscle activity and even if one is unconscious, muscle spasm can occur.

In figure 3.2 is represented an example of raw EEG signal and the filtered one.

4.4.2 Downsampling

For facilitate computing, all data sets were downsampled using the following mne function:

```
> raw = mne.io.read_raw_edf(file).load_data()
> data_resampled = raw.copy().resample(102.4, npad='auto')
```

Usually the sampling factor is based on Nyquist sampling criterion which says that a continuous-time signal can be perfectly reconstructed from its samples if the waveform is sampled over twice as fast as the highest frequency contained in the signal.

$$f_s > 2f_{max}$$

with f_s the sampling frequency (how often samples are taken per unit of time), and f_{max} the highest frequency value.

It is important to notice that no information is lost if sampling above $2f_{max}$ and no information is gained by sampling much faster than that.

For data sets analyzed in this work, according to Nyquist sampling theorem, the sampling rate must be:

$$f_s > 2 * 30$$

hence,

$$f_s > 60$$

since the highest bandwidth (f_{max}) is 30 Hz after band-pass filtering.

In general, it is important to choose enough samples to capture all the peaks and troughs in the signal, otherwise the risk is not only losing information, but getting the wrong information about the signal.

This phenomena takes the name of *aliasing*, that occurs when the signal is sampled at an insufficiently high frequency and some information are lost resulting in a misanalysis.

The result of a generic downsampling is shown in figure 1.11.
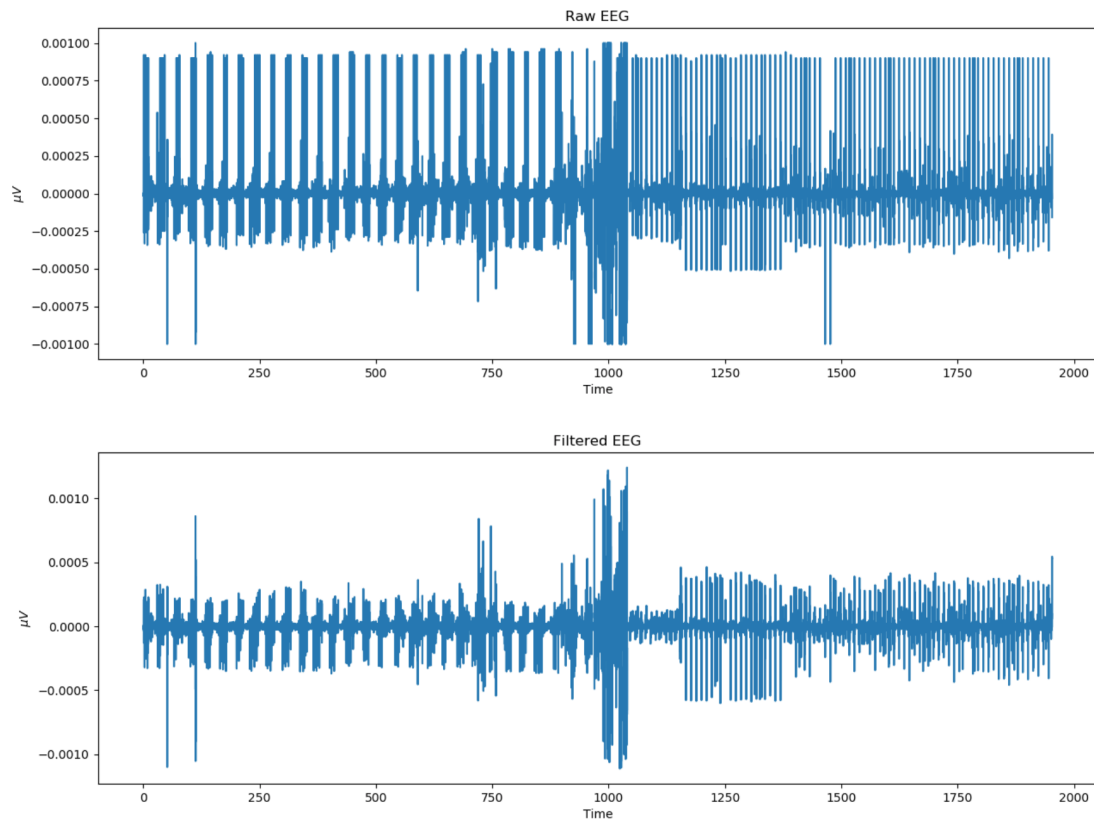
Figure 4.2: Comparison between raw EEG signal and filtered EEG signal. On x-axis is represented the time, on y-axis the amplitude.

4.4.3   Artifact Subspace Reconstruction

Artifact Subspace Reconstruction (ASR) is an online and offline, realtime capable method that can remove artifacts (non-brain signals) which are almost always contained in EEG recordings.

ASR decomposes covariance matrices of the EEG signal to detect artifacts and pursue the goal of reducing or correcting those artifacts.

The ASR algorithm consists of two parts:

- **Calibration:** since ASR depends on the selected data from the signal to calibrate the algorithm, is crucial to select one or more minute long artefact-free segment. This process can be automatically done by the ASR method, making it fully automated.

- **Processing:** each affected time point of the EEG signal is reconstructed from the retained subspace based on the structure observed in calibration data.

The mathematical derivation and technical details of ASR algorithm are available in [43][44].

Even if the effectiveness of ASR and the optimal choice of its parameter have not been evaluated and reported yet, ASR could effectively remove large-amplitude artifacts especially on real EEG data.

4.4.4   Z-score normalization

The last step of this preprocessing phase regards the data normalization. A z-score normalization (also called *standard score*) has been computed in order to be able to make a comparison among subject's EEG time series.

Z-score normalization is a dimensionless quantity obtained by dividing the difference between the value of a sample and the mean of the dataset, and the standard deviation of the dataset.

4.5   Brain connectivity analysis

After preprocessing data, each EEG time serie was splitted in order to extract alpha, beta, delta and theta frequency bands.

Each frequency band was computed individually to be able to extract features from EEG signals. A Granger causality approach was used, considering the causal influence between pairwise channels.

Since G-causality model has 2 important limitations which are the linearity and the stationarity of the model, due to the non-stationarity of biological signals, this model is rejected. However, using Fourier methods, it is possible to examine G-causality in the spectral domain and make then possible a cross-spectral analysis of EEG signals by an AutoRegressive Moving Average model. ARMA model presents the advantage of an immense data reduction since all parameter calculation need only a few parameters.

ARMA model was computed individually for each frequency band, so that the spectral density matrix is generated and the PDC analysis can be done. To facilitate computation, only 8 channels were considered: F3, Fz, F4, C3, Cz, C4, P3 and P4.
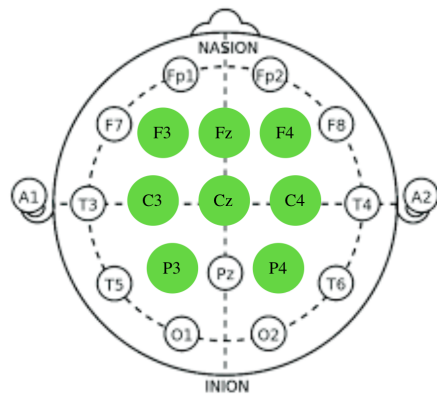
Figure 4.3: In green are shown the 8 selected electrodes on which connectivity analysis was performed.

Connectivity analysis was done considering coupling between distant channels, hence among different brain areas, thus for getting more information on causality:

- P3 → F3 and F3 → P3

- P3 → Fz and Fz → P3

- P3 → F4 and F4 → P3

- P4 → F3 and F3 → P4

- P4 → Fz and Fz → P4

- P4 → F4 and F4 → P4

- C3 → C4 and C4 → C3

4.5.1   Windowing

Once Partial Directed Coherence is obtained, a moving average transform was computed over all PDC dataset. Afterwards, for each pair of channels *i, j* and for each frequency *f*, the moving average was computed and the standard deviation has been calculated.
Windowing was performed on peaks over 1.5 times the standard deviation because small variations $\simeq 0$ are not meaningful for connectivity analysis.
Now the windowing analysis can be done and the following properties are recorded:

- **Number of windows:** the total number of windows that match the condition of having peaks with great variance with respect to the standard deviation. This is because windowing is computed only in case of high connectivity between channels.

- **Average:** the average width (number of samples) for all the computed windows of each couple of channels and each frequency.
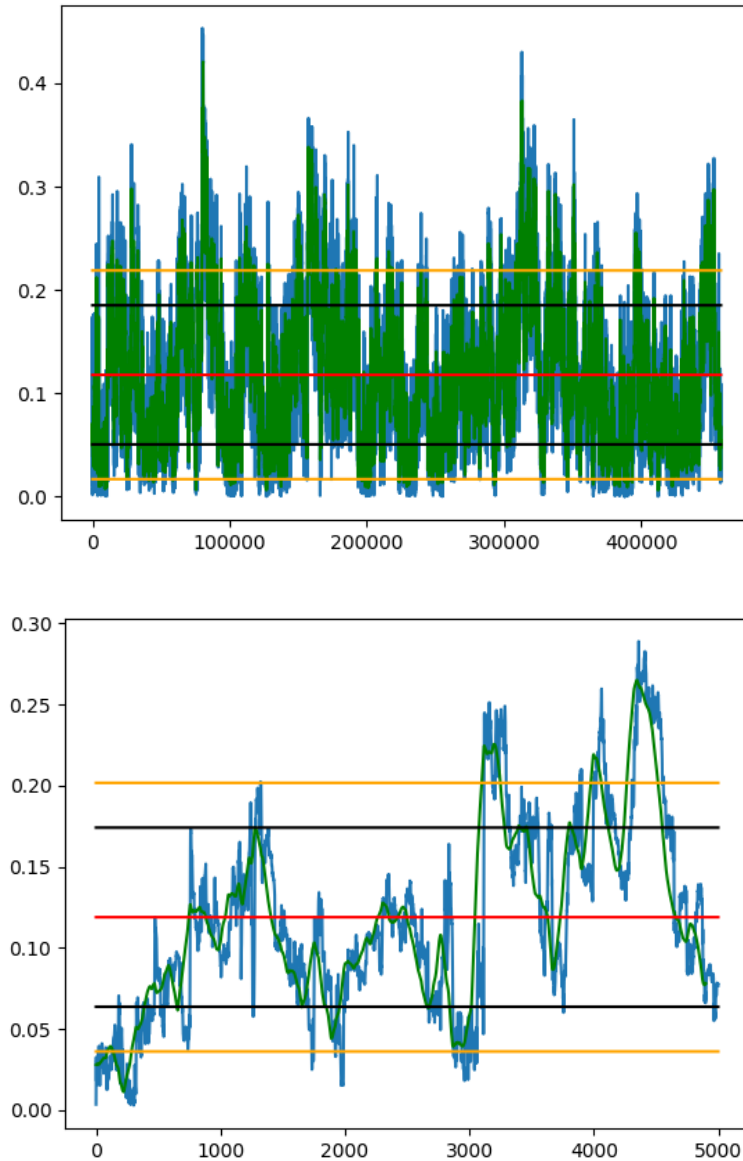
Figure 4.4: Graphical representation of moving average transform.

On x-axes is represented time and on y-axes frequencies.

Blue lines represent original data and in green is represented the moving average. In red is shown the mean, in black the standard deviation between moving average and mean, and in yellow is represented the threshold over which the windowing is computed. At the bottom a zoomed moving average transform.

Chapter 5

Results

In this section are shown some of the most relevant results obtained performing the connectivity analysis on healthy subjects (Hs), DoC patients and a group of patients with some common types of sleep disorders.

A statistical analysis has not been carried out as the analyzed data sample is not large enough for allowing a consistent analysis, indeed results are represented individually for each group of subjects.

5.1 Healthy subjects

Hs - I

In general, as can be seen in the next figures, the connectivity analysis evidences the presence of a high connectivity in alpha and, most of all, in beta frequency bands. This result suggests that individuals were awake and focused during the registration session, since wakefulness is dominated by high-frequency oscillations [45].

The analysis wad performed taking into account different channels for each subject because data sets in [41] contain different number of EEG channels recording (e.g. in Hs - III only 4 channels data were available); but a general observation that may be made regards the neurons preferred direction, which can be easily observed in Hs - I: pair of channels P3 $\rightarrow$ F3 and P3 $\rightarrow$ F4 has

important peaks in contrast to the opposite directions.
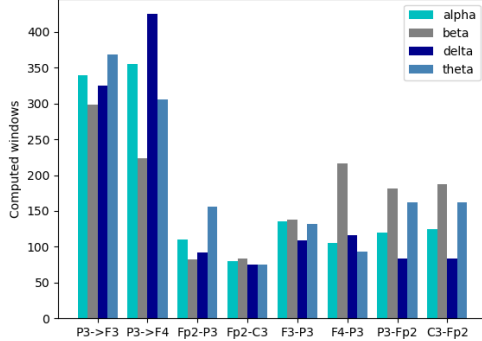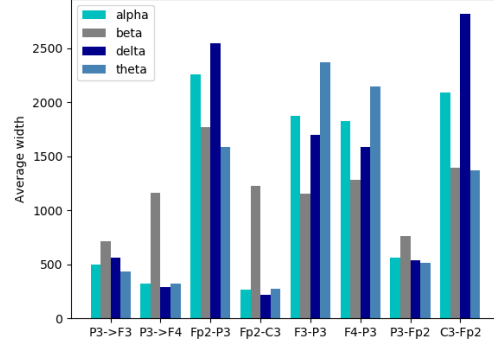
(a) Number of windows   (b) Average window width

Figure 5.1: Connectivity results in Hs - I

Regarding windows width, a general remark concerns the inverse proportionality between the number of windows and their average width: when a high number of windows is detected, their width is smaller and vice-versa.

A great example is given in figure 4.1 for which the higher connectivity in P3 $\rightarrow$ F3 corresponds to a really small-sized windows width.

Hs - II

(a) Number of windows   (b) Number of windows

(c) Average window width

(d) Average window width
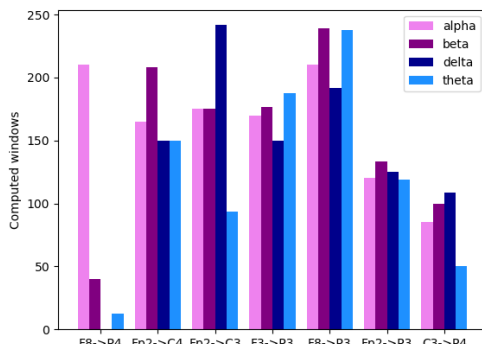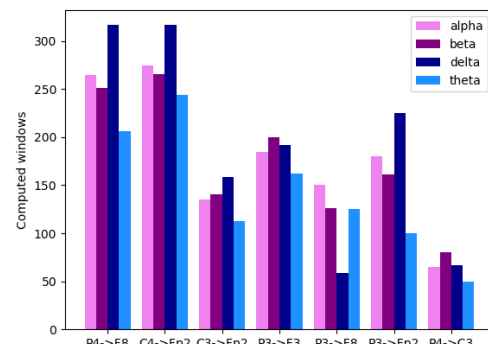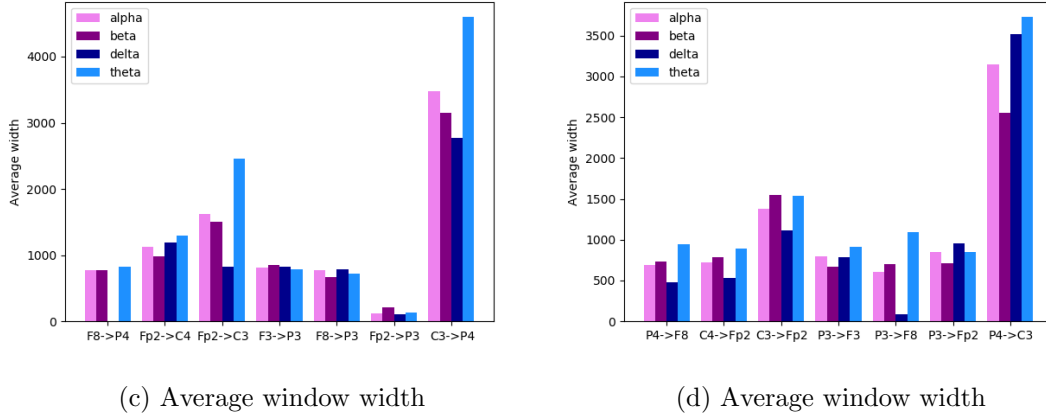
Figure 5.2: Connectivity results in Hs - II

In figure 4.2 are represented results of connectivity analysis done on the second healthy subject. As stated above, a predominance of connectivity is present in a specific direction, this can be observed in fig. 4.2 (a) where Fp2 → C3 and F8 → P3 have higher connectivity with respect to the same channels but in the opposite direction flow (C3 → Fp2 and P3 → F8).

Here again is verified what was said about the inverse proportionality between the number of windows and their average width [fig 4.2 (a,b) vs (c,d)].

Hs - III

The third analyzed healthy subject has EEG recordings arising from only 3 couples of channels.

Some data about the computed number of windows [fig. 4.3 (a)] are not available because presumably some runtime calculation errors has occurred during the connectivity computation.

Instead, the average windows width is shown for all channels pairs in fig. 4.3 (b).

(a) Number of windows

(b) Average window width
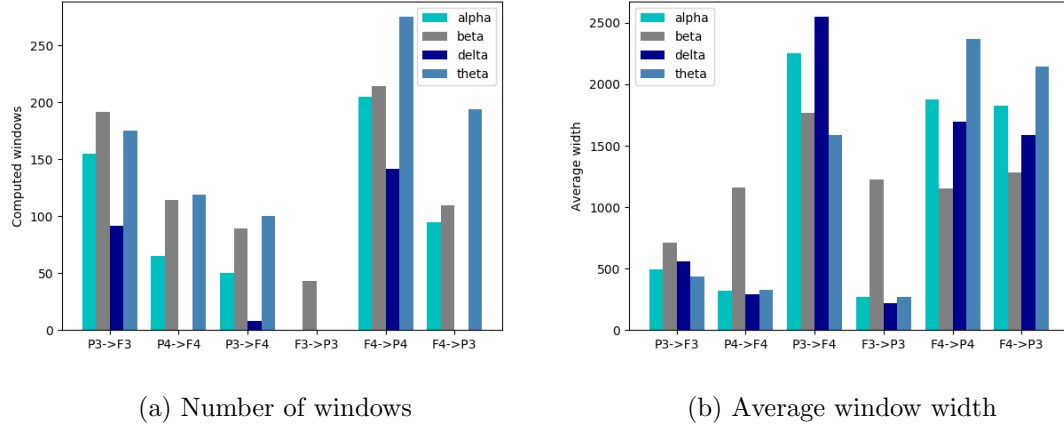
Figure 5.3: Connectivity results in Hs - III

Although the limited number of EEG channels, a general overview of the connectivity trend has been made in healthy subjects, below are shown some interesting connectivity results in patients with consciousness disorders.

5.2   DoC patients

DoC - I

In contrast to EEG recordings in [41], DoC datasets collect recordings from 32 EEG channels positioned according to the standard 10-20 international system.

As was said in section 3.5, the connectivity analysis was performed taking into account only 8 channels because otherwise the computational cost would have been too expensive.

In DoC - I the recording time was approximately 81 minutes and the connectivity results between several pairs of channels are shown in figure 4.4 (a) and (b). In contrast to Hs's connectivity, here the highest connectivity is present in delta and theta frequency bands confirming the person's unconsciousness due to the comatose state.

(a) Number of windows

(b) Number of windows

(c) Average window width

(d) Average window width
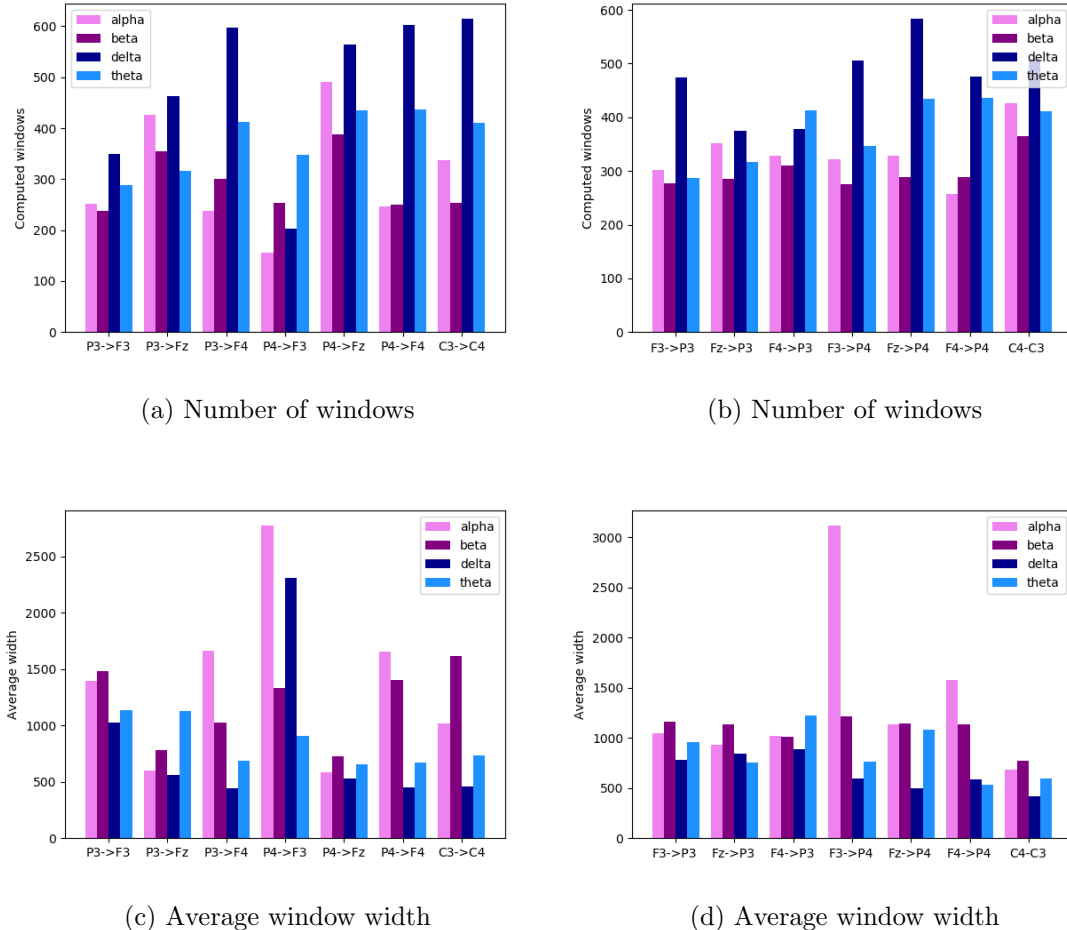
Figure 5.4: Connectivity results in DoC - I

Doc - I is characterized by a general high connectivity for all analyzed channels pair, in particular for couples direction represented in fig 4.4 (b).
The lowest connectivity belongs to P4 → F3 channels but this leads to a major average window width.

In figure 4.5 are represented 3 different curves which indicates in orange the combined features measure which includes permutation entropy, band power value and burst-suppression ratio for state detection, in purple the connectivity between channels F3 → P4 and in green the connectivity be-

tween channels P4 → F3.
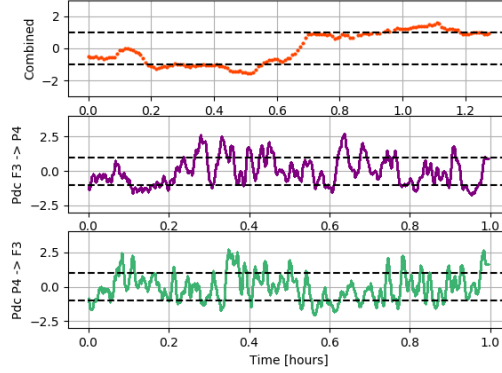
Figure 5.5: Comparison between combined features measure and connectivity values for F3 → P4 and P4 → F3 channels pair in delta frequency band.
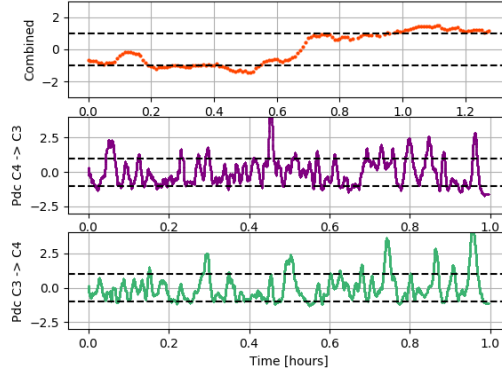
Figure 5.6: Comparison between combined features measure and connectivity values for C3 → C4 and C4 → C3 channels pair in delta frequency band.

The general trend of the combined measures that detects the patient's state is repeated in the connectivity curves trend, this makes it possible to use the connectivity analysis in order to enhance and improve monitoring of the mental state of a DoC patient. In particular, connectivity values arising from channels C3 and C4,

DoC - II

(a) Number of windows

(b) Number of windows

(c) Average window width

(d) Average window width
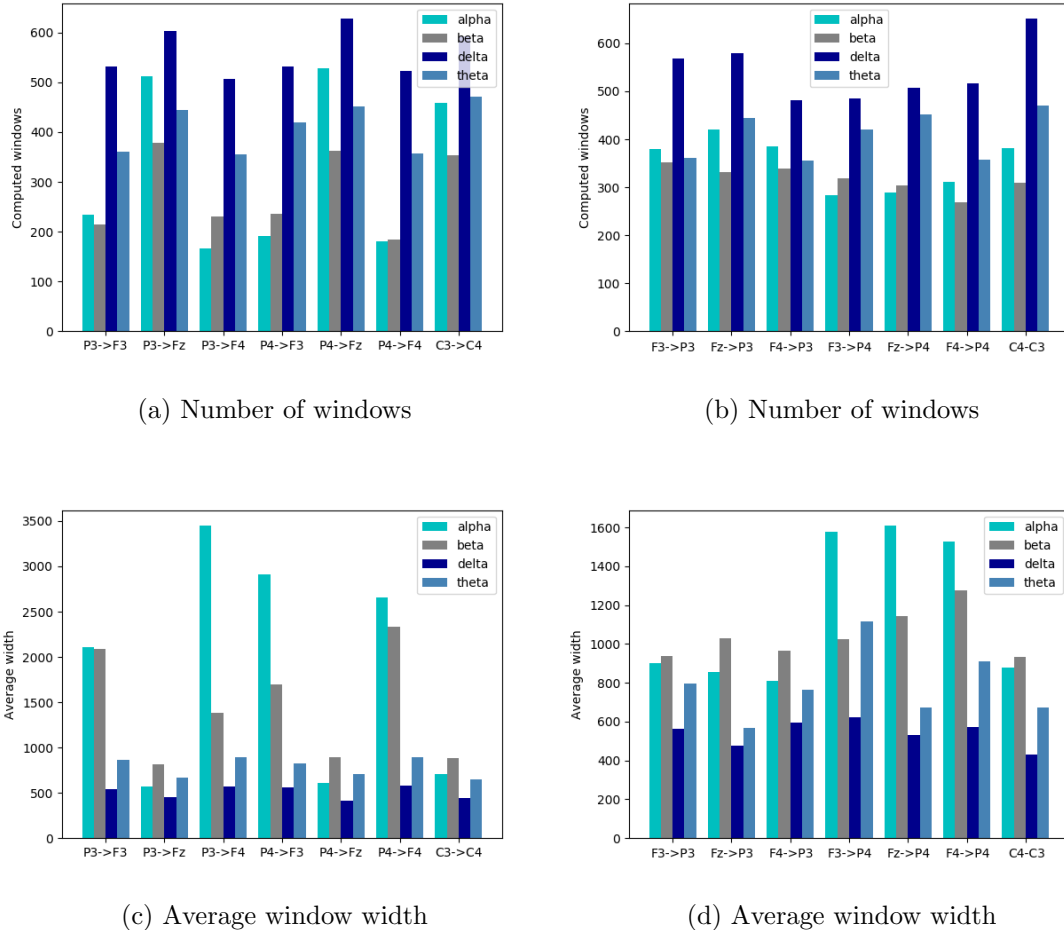
Figure 5.7: Connectivity results in DoC - II

In DoC - II the recording time was approximately 72 minutes and the connectivity results between several pairs of channels are shown in figure 4.6 (a) and (b). As for DoC - I, the connectivity analysis presents a general high connectivity for all analyzed channels pair, in particular for delta frequency band.
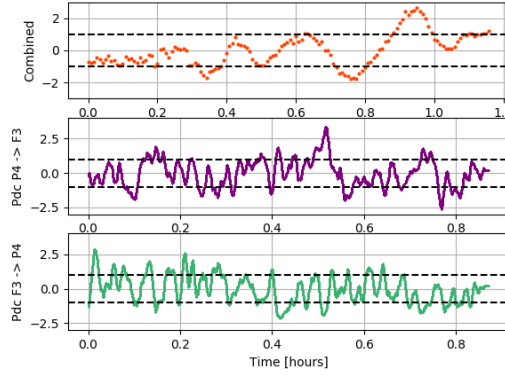
Figure 5.8: Comparison between combined features measure and connectivity values for F3 → P4 and P4 → F3 channels pair in delta frequency band.
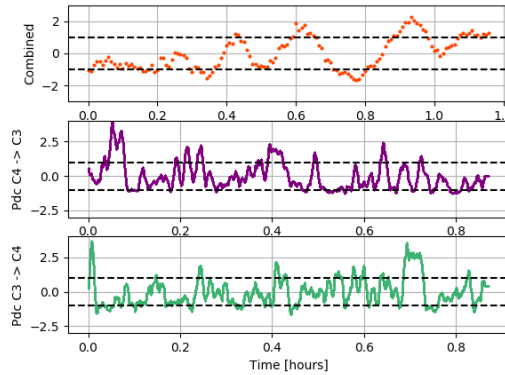
Figure 5.9: Comparison between combined features measure and connectivity values for C3 → C4 and C4 → C3 channels pair in delta frequency band.

Here again the general trend of the combined measures is repeated in the connectivity curves trend, especially in P4 → P3 and C4 → C3. This allows the connectivity analysis to improve and increase the detection of a patient's mental state.

5.3   Other results

In figures 5.10, 5.11 and 5.12 are reported in (a) EEG recordings during sleep of 3 patients with different sleep disorders. Each recording session lasted about 9 hours, but the connectivity analysis was performed only on the first ~58 minutes and results are shown in (b).

What can be assumed from the following graphs is the increased connectivity in channels distant from each other and located in the most central part of the brain, while channels located in the frontal or temporal lobe presents a lower connectivity.

Further analysis should be done in order to investigate the information flow and to complete this results. In particular, for allowing a connectivity comparison among channels, data must be recorded considering the same EEG channels for each patient. This was not possible because for each analyzed data set were not available the same EEG channels recordings, thus only a general assumption was carried out.

5.3.1   Insomnia patient

(a) Sleep stages

(b) Connectivity in delta frequency band
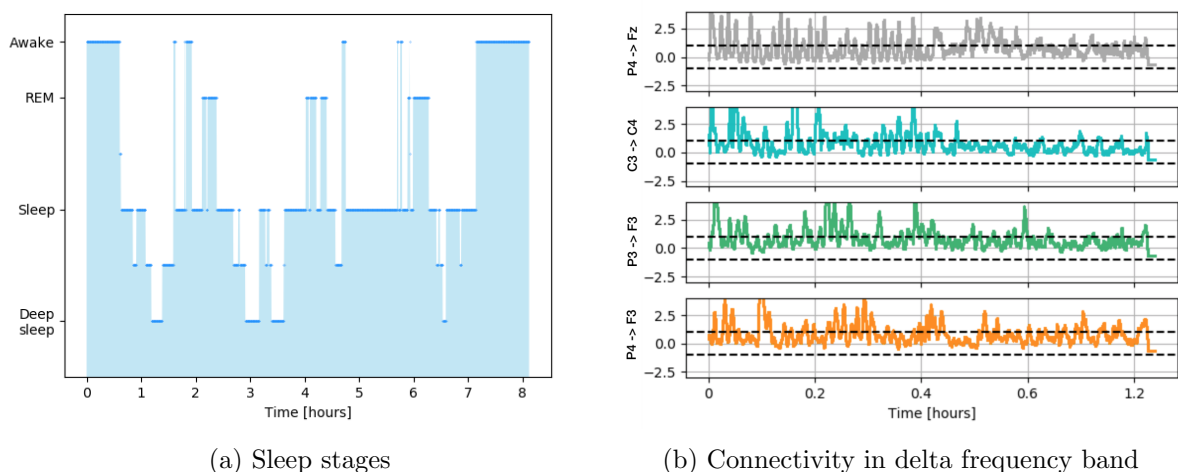
Figure 5.10: Connectivity measures in a insomnia patient.

5.3.2   REM behavior disorder patient

(a) Sleep stages

(b) Connectivity in delta frequency band
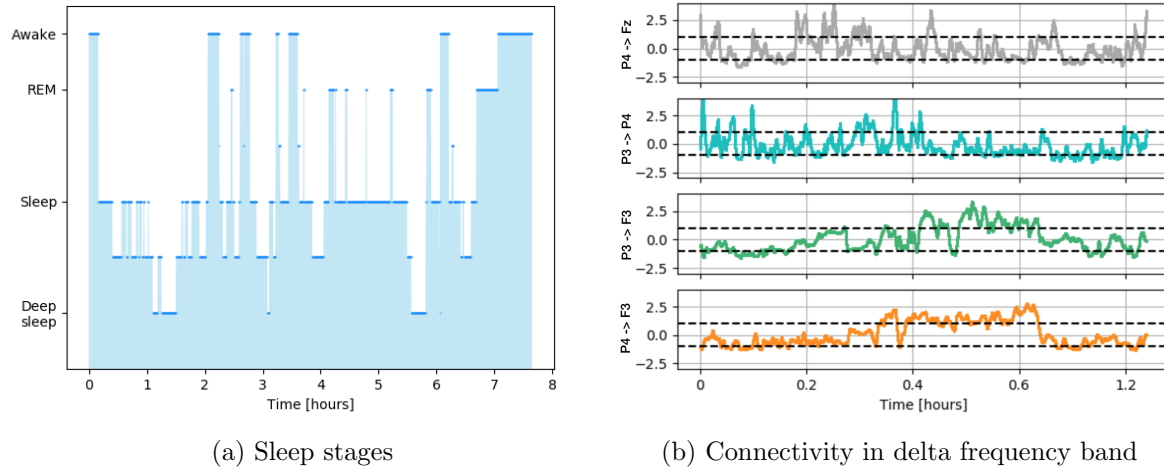
Figure 5.11: Connectivity measures in a REM behavior disorder patient.

5.3.3   Sleep-disordered breathing patient

(a) Sleep stages

(b) Connectivity in delta frequency band
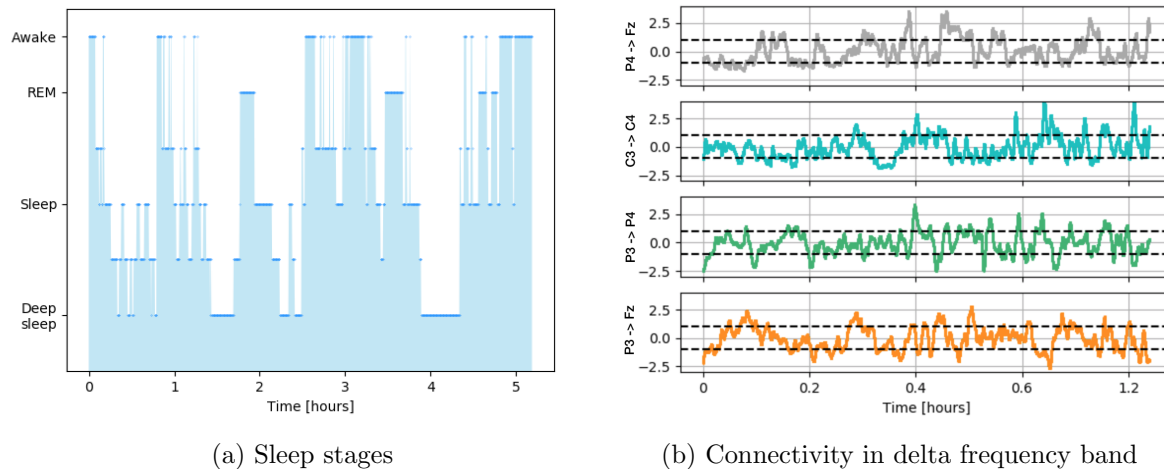
Figure 5.12: Connectivity measures in a sleep-disordered breathing patient.

All three sleep-disordered patients were monitored and data were recorded during a full night of sleep. Results present an irregular sleep cycle that can be easily observed in (a), especially for the REM behavior disorder patient and the sleep-disordered breathing patient.

In fact, they are unable to maintain constant sleep during the night, thus alternating several times wakefulness, REM and sleep phase.

Regarding the connectivity analysis shown in (b), it is possible to establish which coupling of channels have a strong connectivity: pairwise channels P4 $\rightarrow$ Fz which is present in all sleep-disordered patients is characterized by a general high connectivity, but denser in the insomnia patient and less dense in the other two patients.

To investigate this disorders and finding common patterns, much more data are needed, for now we can just say that connectivity analysis can assist and support traditional approaches to make a diagnosis.

Chapter 6

Discussion

6.1 Conclusion

The work presented here has shown that connectivity analysis can be a useful addition to traditional diagnostic approaches used to diagnose different disorders of consciousness.

Even if EEG signals are highly user specific, the functional results deriving from the PDC method can potentially provide additional information for clinical decision makers.

Connectivity studies in healthy subjects, in DoC and in some sleep-disorders patients have led to a better understanding of the processes that are active when the subject lies in different mental states.

For example, healthy subjects presents a high connectivity in alpha-frequencies while in DoC patients there is a predominance of high connectivity in low-frequencies (delta and theta).

However, it is important to highlight the limitations of the connectivity results obtained in this thesis. First of all the number of available channels: DoC recordings and other subjects (healthy and sleep-disordered patients) were recorded taking into account a different number of scalp electrodes. This is a crucial parameter for the performance of EEG source connectivity

methods, in particular it is not possible to make a fair comparison among patients and, especially in healthy subjects, it was not possible to access recordings of electrodes located in the most central part of the brain.

In order to reconstruct brain dynamics and identifying functional connections, much more data should be involved in the connectivity analysis, thus the more electrodes are taken into account, more accurate the analysis will be.

6.2 Future work

Since this analysis has only been conducted in a few individuals, a future work should explore the application of the PDC method and the connectivity analysis to multiply subjects, both healthy, sleep-disordered and DoC patients.

Finally, a comparison between the performance of this connectivity analysis to other functional connectivity analysis methods should be done, in order to identify localized differences in connectivity between healthy controls, DoC patients and other sleep-disorder pathologies.

Bibliography

[1] K. R. Van Dijk, T. Hedden, A. Venkataraman, K. C. Evans, S. W. Lazar, R. L. Buckner. "Intrinsic Functional Connectivity As a Tool For Human Connectomics: Theory, Properties, and Optimization". Journal of Neurophysiology, 2010.

[2] http://learn.neurotechedu.com/introtobci/

[3] L. Vincent, G.H. Patel, M.D. Fox, A.Z. Snyder, J.T. Baker, D.C. Van Essen, J.M. Zempel, L.H. Snyder, M. Corbetta, M.E. Raichle. "Intrinsic functional architecture in the anesthetized monkey brain". Nature, 2007.

[4] R. M. Hutchison, T. Womelsdorf, E. A. Allen, P. A. Bandettini, V. D. Calhoun, M. Corbetta, S. Della Penna, J. H. Duyn, G. H. Glover, J. Gonzalez-Castillo, D. A. Handwerker, S. Keilholz, V. Kiviniemi, D.A. Leopold, F. De Pasquale, O. Sporns, M. Walter, C. Chang. "Dynamic functional connectivity: Promise, issues, and interpretations". NeuroImage, 2003.

[5] K. J. Friston. "Functional and Effective Connectivity in Neuroimaging: A Synthesis". Human Brain Mapping, 1994.

[6] W. Majeed, M. Magnuson, S. D. Keilholz. "Spatiotemporal dynamics of low frequency fluctuations in BOLD fMRI of the rat". Journal of Magnetic Resonance Imaging, 2009.

[7] W. Majeed, M. Magnuson, W. Hasenkamp, H. Schwarb, E. H. Schumacher, L. Barsalou, S. D.Keilholz. "Spatiotemporal dynamics of low frequency BOLD fluctuations in rats and humans". NeuroImage, 2011.

[8] E. Tagliazucchi, P. Balenzuela, D. Fraiman, D. Chialvo, R. Dante. "Criticality in large-scale brain fMRI dynamics unveiled by a novel point process analysis". Frontiers in Physiology, 2012.

[9] E. Tagliazucchi, M. Siniatchkin, H. Laufs, D. R. Chialvo. "The voxel-wise functional connectome can be efficiently derived from co-activations in a sparse spatio-temporal point-process". Frontiers in Neuroscience, 2016.

[10] M. E. Raichle, A. Z. Snydera. "A default mode of brain function: A brief history of an evolving idea". Elsevier, 2007.

[11] I. W. Renner, J. Elith, A. Baddeley, W. Fithian, T. Hastie, S. J. Phillips, G. Popovic, D. I. Warton. "Point process models for presence-only analysis". Methods in Ecology and Evolution, 2015.

[12] M. D. Greicius, K. Supekar, V. Menon, R. F. Dougherty. "Resting-state functional connectivity reflects structural connectivity in the default mode network". Cerebral cortex, 2009.

[13] G. Bartzokis, J. L. Cummings, D. Sultzer, V. W. Henderson, K. H. Nuechterlein, J. Mintz. "White matter structural integrity in healthy aging adults and patients with Alzheimer disease: a magnetic resonance imaging study". Archives of neurology, 2003.

[14] P. Hagmann, O. Sporns, N. Madan, L. Cammoun, R. Pienaar, V. J. Wedeen, R. Meuli, J. P. Thiran, P. E. Grant. "White matter maturation reshapes structural connectivity in the late developing human brain". Proceedings of the National Academy of Sciences of the United States of America, 2010.

[15] D. Cordes, V. M. Haughton, J. D. Carew, K. Arfanakis, K. Maravilla. "Hierarchical clustering to measure connectivity in fMRI resting-state data". Magnetic Resonance Imaging, 2002.

[16] S. Laureys. "The neural correlate of (un)awareness: lessons from the vegetative state". Trends In Cognitive Sciences, 2005.

[17] A. E. Cavanna, S. Shah, C. M. Eddy, A. Williams, H. Rickards. "Consciousness: A neurological perspective". Behavioural Neurology, 2011.

[18] S. Laureys, G. G. Celesia, F. Cohadon, J. Lavrijsen, J. Leon-Carrion, W. G. San- nita, L. Sazbon, E. Schmutzhard, K. R. von Wild, A. Zeman, G. Dolce. "Un-responsive wakefulness syndrome: a new name for the vegetative state or apallic syndrome". Bmc Medicine, 2010.

[19] https://en.wikipedia.org/wiki/Glasgow_Coma_Scale

[20] C. Schnakers, A. Vanhaudenhuyse, J. Giacino, M. Ventura, M. Boly, S. Majerus, G. Moonen, S. Laureys. "Diagnostic accuracy of the vegetative and minimally conscious state: Clinical consensus versus standardized neurobehavioral assessment". Bmc Neurology, 2009.

[21] M. M. Monti, S. Laureys, A. M. Owen. "The vegetative state". British Medical Journal, 2010.

[22] M. H. Davis, M. R. Coleman, A. R. Absalom, J. M. Rodd, I. S. Johnsrude, B. F. Matta, A. M. Owen, D. K. Menon. "Dissociating speech perception and comprehension at reduced levels of awareness". Proceedings of the National Academy of Sciences of the United States of America, 2007.

[23] A. M. Owen, M. R. Coleman, M. Boly, M. H. Davis, S. Laureys, J. D. Pickard. "Detecting awareness in the vegetative state". Science, 2006.

[24] E. Niedermeyer, F. L. Da Silva. "Electroencephalography: Basic Principles, Clinical Applications, and Related Fields". Urban and Schwarzenberg, 1982.

[25] https://www.rednewswire.com/global-electroencephalogram-system/

[26] A. Brovelli. "Basi fisiologiche dei segnali biologici complessi". Università degli Studi di Trieste, 2012.

[27] N. Bigdely-Shamlo, T. R. Mullen, C. Kothe, K. Su, K. Robbins. "The PREP Pipeline: Standardized preprocessing for large-scale EEG analysis". Frontiers in Neuroinformatics, 2015.

[28] F. Lotte, L. Bougrain, A. Cichocki, M. Clerc, M. Congedo, A. Rakotomamonjy, F. Yger. "A Review of Classification Algorithms for EEG-based Brain-Computer Interfaces: A 10-year Update". Hal, 2018.

[29] D. Mantini, S. Della Penna,L. Marzetti, F. De Pasquale, V. Pizzella, Ma. Corbetta, G. L. Romani. "A Signal-Processing Pipeline for Magnetoencephalography Resting-State Networks". Brain connectivity, 2011.

[30] M. West, R. Prado, A. D. Krystal. "Evaluation and comparison of EEG traces: latent structure in nonstationary time series". Journal of the American Statistical Association, 1999.

[31] S. Parsons, A. M. Boonman, M. K. Obrist. "Advantages and Disadvantages of Techniques for Transforming and Analyzing Chiropteran Echolocation Calls". Journal of Mammalogy, 2000.

[32] Wolfram Hesse, Eva Moller, Matthias Arnold, Barbel Schack. "The use of time-variant EEG Granger causality for inspecting directed interdependencies of neural assemblies". Journal of Neuroscience, 2003.

[33] https://en.wikipedia.org/wiki/Granger_causality

[34] R. Shriram, M. Sundhararajan, N. Daimiwal. "Brain Connectivity Analysis Methods for Better Understanding of Coupling". International Journal of Computer Science and Information Security, 2012.

[35] S. Fazli, J. Mehnert, J. Steinbrink, G. Curio, A. Villringer, K. R. MÃ¼ller, B. Blankertz. "Enhanced Performance By A Hybrid NIRS-EEG Brain Computer Interface". NeuroImage, 2012.

[36] G. Mele, C. Cavaliere, V. Alfano, M. Orsini, M. Salvatore, M. Aiello. "Simultaneous EEG-fMRI for Functional Neurological Assessment". Frontiers in Neurology, 2019.

[37] K. Blinowska, G. Putz, V. Kaiser, L. Astolfi, K. Vanderperren, S. Van Huffel, L. Lemieux "Multimodal Imaging of Human Brain Activity: Rational, Biophysical Aspects and Modes of Integration". Computational Intelligence and Neuroscience, 2009.

[38] S. Merz. "Functional connectivity in disorders of consciousness". Eberhard-Karls-University Tubingen.

[39] S. Evangelisti. "An fMRI study of brain functional connectivity in Parkinson's disease patients". University of Bologna.

[40] A. Zhigalov, "Time series analysis in neuroscience", Dept. of CS, University of Helsinki and Dept. of NBE, Aalto University.

[41] https://www.physionet.org/content/capslpdb/1.0.0/

[42] https://mne.tools/stable/index.html

[43] C. A. E. Kothe, T. P. Jung. "Artifact removal techniques with signal reconstruction". U.S. Patent Application, 2014.

[44] T. R. Mullen, C. A. Kothe, M. Chi, A. Ojeda, T. Kerth, S. Makeig, T. P. Jung, G. Cauwenberghs. "Real-time neuroimaging and cognitive monitoring using wearable dry eeg". IEEE Trans. on Biomed. Eng., 2015.

[45] `https://raphaelvallat.com/bandpower.html`

Connectivity results on DoC patients

Table A.1:

Total samples: 427812

channels		P3 → F3		P3 → Fz		P3 → F4		P4 → F3		P4 → Fz		P4 → F4		C3 → C4	
		n.win	avg	n.win	avg	n.win	avg	n.win	avg	n.win	avg	n.win	avg	n.win	avg
freq	8	342	741.92	465	430.87	406	705.89	362	681.67	508	367.01	352	827.49	455	561.53
	9	388	758.90	543	467.84	367	856.54	370	800.92	472	551.99	337	934.06	408	804.60
	10	344	1040.91	476	593.20	341	975.99	345	1011.93	404	812.04	329	1025.11	346	1023.68
	11	381	799.91	383	641.51	368	760.30	382	749.21	342	862.66	373	796.35	389	740.19
	12	249	1297.06	311	805.96	231	1261.92	257	1149.66	290	849.39	202	1758.31	284	1101.00
	13	318	904.47	417	494.07	269	1222.79	358	877.15	434	453.55	156	2475.28	321	907.57
	14	337	891.29	473	527.29	283	1181.74	335	960.95	467	495.59	164	2380.10	336	920.54
	15	326	974.04	418	707.66	260	1295.4	328	926.18	471	597.32	169	2281.3	312	1060.3
	16	333	938.61	362	854.91	326	976.30	343	897.02	403	727.75	247	1411.8	364	828.21
	17	343	808.79	341	840.12	370	783.53	369	806.33	360	818.56	333	848.48	314	862.81
	18	260	1010.74	243	1128.53	309	914.07	318	858.39	320	923.51	259	1098.97	254	1181.07
	19	233	1152.97	213	1320.29	209	1416.51	234	1089.78	270	1070.43	150	2152.74	166	1925.53
	20	183	1560.69	219	1315.97	171	1895.16	212	1279.32	246	1117.34	138	2593.87	142	2267.52
	21	342	828.39	418	630.23	284	1148.0	362	745.32	378	566.00	274	1277.6	323	922.75
	22	379	770.00	384	795.30	283	1186.0	333	853.25	368	703.72	286	1192.1	345	899.28
	23	355	742.69	418	687.10	323	975.73	373	776.11	334	839.03	365	823.86	370	786.18
	24	307	770.63	344	745.77	298	900.12	312	848.21	343	766.48	334	793.55	356	716.61
	25	227	1105.58	267	1005.88	207	1239.17	262	1032.77	246	1009.45	227	1343.28	227	1169.85
	26	315	901.91	392	554.14	275	1155.2	352	861.73	395	549.57	213	1689.7	331	787.31
	27	289	1019.0	392	659.58	292	1123.3	337	908.65	347	715.80	254	1407.9	351	792.57
	28	324	917.58	357	703.98	310	962.76	335	843.91	364	683.21	342	925.22	339	856.76
	29	354	857.91	302	811.57	329	799.10	310	859.88	311	772.13	340	810.59	357	793.80
	30	218	1404.08	260	1056.95	254	1053.89	286	989.318	259	1012.96	259	1081.86	264	1055.50

channels		F3 → P3		Fz → P3		F4 → P3		F3 → P4		Fz → P4		F4 → P4		C4 → C3	
		n.win	avg	n.win	avg	n.win	avg	n.win	avg	n.win	avg	n.win	avg	n.win	avg
freq	8	409	677.38	397	677.41	356	697.14	404	586.76	466	534.98	431	515.81	489	395.92
	9	344	928.39	398	778.33	398	690.29	427	732.71	419	758.27	434	635.00	548	482.12
	10	327	1057.59	391	873.12	394	811.70	293	1234.72	323	1081.46	333	1012.75	416	770.312
	11	338	919.40	359	897.84	338	841.55	331	1008.20	343	921.05	313	977.78	383	721.67
	12	212	1660.32	201	1825.75	259	1177.94	261	1269.01	222	1587.62	219	1470.71	271	1012.98
	13	341	765.57	358	776.27	359	657.52	385	700.98	387	713.46	370	755.80	415	519.81
	14	356	767.25	366	798.57	340	758.97	348	880.91	374	796.21	353	833.38	391	681.56
	15	321	916.95	335	947.67	322	877.11	299	1096.1	341	918.87	342	906.31	372	850.81
	16	378	750.53	361	845.03	352	796.30	310	1020.92	359	839.55	379	769.23	321	1033.55
	17	324	770.85	326	821.75	338	744.43	329	885.52	331	868.00	365	734.13	328	915.95
	18	224	1229.0	259	1135.0	270	1016.2	212	1424.3	230	1347.0	264	1087.5	288	993.33
	19	195	1599.45	184	1646.47	215	1423.73	170	1806.42	181	1735.20	222	1310.04	271	1063.01
	20	148	2207.53	179	1729.03	192	1662.91	186	1509.37	193	1654.09	238	1218.45	258	1017.55
	21	312	1024.65	335	882.23	347	810.36	362	701.98	343	720.60	374	696.97	468	583.14
	22	288	1163.98	309	1010.29	332	914.83	323	798.86	357	754.56	418	673.59	353	875.01
	23	339	909.37	341	863.98	371	736.64	328	746.66	387	710.28	383	702.63	335	887.01
	24	336	765.53	301	901.29	309	797.95	275	984.92	381	635.97	337	697.46	341	795.78
	25	262	1023.30	219	1292.87	232	1173.03	202	1460.68	273	944.26	259	961.71	268	1036.70
	26	321	940.62	345	717.33	336	840.82	315	780.78	347	834.87	415	653.20	394	523.88
	27	333	922.46	317	868.51	327	949.25	329	804.24	324	950.33	353	840.57	415	703.75
	28	361	811.12	323	877.66	330	839.59	357	703.26	352	827.08	389	716.88	390	805.47
	29	346	695.92	288	949.57	312	752.14	299	796.37	299	876.36	293	812.24	310	890.61
	30	244	1064.6	222	1303.6	219	1246.3	243	1113.6	255	1145.8	239	1119.3	285	955.55

Table A.2:

Total samples: 453207

channels		P3 → F3		P3 → Fz		P3 → F4		P4 → F3		P4 → Fz		P4 → F4		C3 → C4	
		n.win	avg	n.win	avg	n.win	avg	n.win	avg	n.win	avg	n.win	avg	n.win	avg
freq	20	298	652,87	348	799,15	418	626,82	301	739,16	397	584,70	343	676,30	456	443,53
	21	320	690,6	367	810,44	415	704,88	286	803,95	408	644,60	347	763,26	478	502,79
	22	303	880,25	336	982,13	423	751,27	304	784,86	377	829,90	356	803,87	418	669,86
	23	340	824,64	349	946,54	394	737,35	339	721,58	358	851,26	371	794,52	426	656,77
	24	361	815,55	338	862,17	340	775,14	329	830,51	321	806,66	333	918,36	354	815,20
	25	231	1426,06	243	1283,02	290	1016,23	268	1059,28	255	111,02	202	1809,46	290	1015,15
	26	304	947,62	339	854,34	326	721,40	265	930,79	313	883,84	318	582,61	344	810,06
	27	254	1272,47	335	962,65	366	788,16	245	1050,37	333	946,80	354	652,29	355	923,30
	28	298	1022,28	361	902,03	351	894,01	312	904,06	316	1032,43	307	938,20	369	897,77
	29	283	942,20	318	894,88	325	939,33	302	881,11	310	973,20	318	887,73	338	901,71
	30	235	1362,44	262	989,82	276	1036,81	243	1232,65	256	1145,45	256	1142,51	303	1000,41

channels		F3 → P3		Fz → P3		F4 → P3		F3 → P4		Fz → P4		F4 → P4		C4 → C3	
		n.win	avg	n.win	avg	n.win	avg	n.win	avg	n.win	avg	n.win	avg	n.win	avg
freq	20	282	1319,59	255	1421,09	268	1324,55	34	8155,35	54	8058,66	37	11279,21	292	898,54
	21	284	1321,13	245	1431,56	273	1320,11	24	11652,62	36	12151,05	35	10146,94	302	800,80
	22	345	1001,57	265	1344,58	266	1338,84	57	7307,10	37	11761,97	66	6567,83	289	1060,13
	23	325	659,64	331	916,80	376	790,38	201	1981,47	196	1852,28	263	1366,15	334	916,25
	24	254	649,76	408	670,43	355	719,18	325	752,16	293	748,82	290	901,07	304	957,88
	25	219	1250,30	267	1101,53	238	1230,22	231	1161,19	236	1285,16	181	1835,86	251	1097,12
	26	154	2632,82	241	1598,90	183	2054,12	163	2453,25	88	4822,59	49	8759,18	309	1014,83
	27	241	1602,19	237	1634,41	178	2123,86	189	2052,62	108	3934,21	117	3551,83	260	1220,4
	28	323	710,43	301	1062,76	299	1086,24	257	1205,77	196	1989,92	240	1462,93	308	1017,03
	29	251	677,70	313	761,42	338	790,60	247	942,53	269	1219,86	299	958,47	354	765,37
	30	215	1180,31	277	1039,51	267	1177,09	211	1248,16	226	1347,70	231	1347,02	267	1023,61

Table A.3:

Total samples: 458225

channels		P3 → F3		P3 → Fz		P3 → F4		P4 → F3		P4 → Fz		P4 → F4		C3 → C4	
		n.win	avg	n.win	avg	n.win	avg	n.win	avg	n.win	avg	n.win	avg	n.win	avg
freq	1	424	505,11	584	326,38	448	464,51	468	589,81	577	368,77	497	499,93	622	318,66
	2	440	526,95	634	368,14	463	529,21	476	610,69	651	392,21	509	513,00	657	363,07
	3	472	564,38	606	449,87	458	622,47	431	714,73	573	529,16	525	538,00	649	462,20
	4	476	618,21	500	542,45	475	623,93	452	639,35	506	612,04	495	604,56	567	540,20
	5	357	849,66	417	738,25	355	863,82	220	1528,75	384	883,84	487	594,77	544	515,77
	6	358	834,62	421	706,80	336	864,26	247	1368,99	343	975,42	481	638,58	471	591,67
	7	372	791,87	408	664,95	360	739,06	310	966,11	377	826,90	483	575,00	416	615,92
	8	377	798,09	326	852,83	311	885,36	299	948,10	381	766,34	413	650,19	394	679,53

channels		F3 → P3		Fz → P3		F4 → P3		F3 → P4		Fz → P4		F4 → P4		C4 → C3	
		n.win	avg	n.win	avg	n.win	avg	n.win	avg	n.win	avg	n.win	avg	n.win	avg
freq	1	529	344,95	620	309,35	520	369,14	483	402,68	588	335,26	605	292,65	449	393,61
	2	549	425,43	616	397,63	550	401,10	547	398,92	640	385,67	637	346,60	498	405,63
	3	505	546,06	549	509,00	542	467,15	589	441,19	552	534,66	597	449,51	502	465,15
	4	516	577,15	520	539,44	530	539,07	561	520,46	535	588,20	577	500,72	461	527,70
	5	414	854,80	545	499,75	460	597,32	473	615,59	469	589,30	402	780,26	442	523,58
	6	364	960,53	461	562,94	436	619,20	435	660,03	431	663,35	376	832,10	388	589,36
	7	395	783,82	403	601,53	464	537,15	375	690,03	426	643,06	348	841,14	339	686,35
	8	338	831,49	374	665,60	402	635,53	463	406,70	397	668,72	337	849,42	340	757,17

Table A.4:

Total samples: 266020

channels		P3 → F3		P3 → Fz		P3 → F4		P4 → F3		P4 → Fz		P4 → F4		C3 → C4	
		n.win	avg	n.win	avg	n.win	avg	n.win	avg	n.win	avg	n.win	avg	n.win	avg
freq	1	211	751.72	270	344.58	176	754.61	252	455.96	295	430.42	149	1317.3	201	550.08
	2	220	715.86	246	439.01	203	684.77	262	511.03	282	593.55	155	1320.2	222	511.69
	3	230	665.47	198	553.65	224	703.24	238	660.64	219	810.40	179	1045.0	220	460.22
	4	262	586.42	150	682.18	196	648.39	232	650.19	198	758.92	177	706.58	222	451.93

channels		F3 → P3		Fz → P3		F4 → P3		F3 → P4		Fz → P4		F4 → P4		C4 → C3	
		n.win	avg	n.win	avg	n.win	avg	n.win	avg	n.win	avg	n.win	avg	n.win	avg
freq	1	270	517.64	325	362.29	268	544.70	279	386.81	293	450.93	216	543.16	261	363.47
	2	242	575.56	367	395.83	296	538.95	308	440.88	302	492.16	252	519.35	298	373.69
	3	232	548.93	332	432.45	262	590.94	282	596.07	277	541.47	301	504.52	248	521.85
	4	233	496.76	223	447.48	239	473.88	248	631.97	227	500.48	281	538.24	174	691.10

Table A.5:

Total samples: 52107

channels		P3 → F3		P3 → Fz		P3 → F4		P4 → F3		P4 → Fz		P4 → F4		C3 → C4	
		n.win	avg	n.win	avg	n.win	avg	n.win	avg	n.win	avg	n.win	avg	n.win	avg
freq	1	44	393.29	43	604.02	41	861.68	42	936.14	13	1318.61	42	501.09	27	1401.25
	2	44	496.97	37	883.40	35	906.00	32	774.03	17	1064.2	36	592.55	28	1289.2
	3	35	529.51	36	979.97	41	684.21	21	946.28	16	1339.2	34	702.14	19	1811.1
	4	39	811.58	29	1137.1	44	705.43	31	900.09	16	1478.8	23	920.86	35	930.88

channels		F3 → P3		Fz → P3		F4 → P3		F3 → P4		Fz → P4		F4 → P4		C4 → C3	
		n.win	avg	n.win	avg	n.win	avg	n.win	avg	n.win	avg	n.win	avg	n.win	avg
freq	1	28	659.60	69	410.63	56	295.80	38	430.15	63	383.47	62	429.30	1	213.00
	2	32	581.00	60	553.25	56	473.80	39	522.48	66	421.83	52	396.73	2	2312.0
	3	31	676.90	65	495.58	39	779.12	42	995.73	58	455.46	41	394.19	16	641.37
	4	33	946.21	56	565.23	34	830.79	28	805.17	41	513.24	38	499.78	26	391.73

Table A.6:

Total samples: 471230

channels		P3 → F3		P3 → Fz		P3 → F4		P4 → F3		P4 → Fz		P4 → F4		C3 → C4	
		n.win	avg	n.win	avg	n.win	avg	n.win	avg	n.win	avg	n.win	avg	n.win	avg
freq	13	99	4354.40	305	1007.79	154	2739.14	110	3837.70	401	685.50	269	1463.5	564	366.06
	14	88	4913.54	301	1031.7	108	3835.4	79	5413.05	389	751.20	219	1893.9	534	548.01
	15	100	4270.4	293	1152.3	138	2753.5	64	7063.29	355	933.39	190	2189.5	418	825.73
	16	255	1511.80	307	1145.87	221	1723.07	168	2529.54	400	879.38	304	1205.83	371	889.69
	17	309	928.66	348	842.439	296	1146.80	286	1040.78	383	797.11	335	967.98	324	898.55
	18	234	1446.48	274	1049.22	248	1354.86	222	1413.04	305	998.39	215	1662.09	254	1135.47
	19	142	2750.76	216	1257.92	161	2046.57	166	2130.99	251	1365.21	146	2580.92	279	1069.76
	20	111	3700.94	227	1182.21	156	2324.03	142	2709.78	259	1368.11	110	3399.99	274	1121.96
	21	48	7243.60	301	1018.96	276	1090.68	60	7656.85	326	836.36	274	1213.58	457	634.67
	22	52	7073.11	292	1151.98	319	984.19	82	5343.07	300	971.33	270	1397.88	425	790.13
	23	202	2006.38	320	1013.91	341	932.01	170	2410.35	373	839.57	268	1425.13	446	676.12
	24	332	904.59	316	814.17	368	852.201	300	1089.44	330	889.66	352	926.69	368	735.57
	25	230	1555.84	258	1094.23	269	1134.94	218	1516.37	281	1201.79	260	1249.19	275	1080.79

channels		F3 → P3		Fz → P3		F4 → P3		F3 → P4		Fz → P4		F4 → P4		C4 → C3	
		n.win	avg	n.win	avg	n.win	avg	n.win	avg	n.win	avg	n.win	avg	n.win	avg
freq	13	51	8191.56	19	22328.57	42	9999.04	108	3345.62	288	1067.32	208	1769.78	322	819.28
	14	36	11679.11	19	22398.47	43	9821.09	74	4414.41	238	1449.03	184	2154.11	372	812.32
	15	51	8216.82	27	15702.70	54	7782.81	83	3438.42	184	2038.23	136	2983.30	351	998.10
	16	190	2185.68	140	2976.85	103	4072.34	158	2340.56	260	1327.57	205	1783.38	384	907.82
	17	344	944.63	327	1058.19	297	1120.86	271	1084.73	295	908.857	282	1003.43	332	952.469
	18	189	1851.20	179	2025.66	222	1438.61	266	1097.21	246	1216.56	187	1811.07	289	1137.89
	19	132	2614.69	107	3747.88	136	2648.98	178	1902.25	162	1988.70	128	2928.61	262	1173.24
	20	102	3842.07	75	5710.29	85	4786.00	122	3327.09	158	2214.63	111	3366.55	241	1210.80
	21	174	2464.56	210	1709.19	91	4230.63	173	2067.62	272	1060.42	318	906.16	324	945.89
	22	169	2450.33	175	2257.71	95	4419.63	219	1735.74	238	1450.71	342	943.38	303	1097.99
	23	262	1362.08	246	1536.40	188	2232.04	263	1364.49	263	1420.02	330	937.35	377	888.65
	24	305	970.31	336	875.90	328	916.02	315	1031.80	276	1167.05	323	871.12	323	1061.10
	25	238	1363.46	254	1296.73	250	1397.09	232	1509.95	205	1598.15	241	1287.03	241	1452.89

Table A.7:

Total samples: 470615

channels		P3 → F3		P3 → Fz		P3 → F4		P4 → F3		P4 → Fz		P4 → F4		C3 → C4	
		n.win	avg	n.win	avg	n.win	avg	n.win	avg	n.win	avg	n.win	avg	n.win	avg
freq	1	555	459,94	668	297,19	584	449,32	468	375,06	662	307,38	554	440,90	583	372,18
	2	545	546,93	629	413,31	597	489,55	556	386,69	668	392,67	597	440,90	604	398,93
	3	478	673,94	544	506,04	612	511,26	533	486,20	530	540,94	570	527,92	615	466,77
	4	471	570,63	453	518,63	571	466,44	514	489,62	487	545,43	571	538,30	587	518,98
	8	118	1922,76	192	1300,09	135	1488,36	166	1714,89	227	1437,48	155	1996,76	210	1430,07
	9	132	1632,68	221	1138,40	174	1249,80	210	1332,7	207	1442,42	191	1510,30	230	1355,38
	10	191	1216,59	224	1137,36	282	891,13	229	1180,33	214	1393,57	242	1159,03	235	1420,62
	11	230	1102,11	218	1195,23	239	1225,43	194	1409,01	211	1372,82	279	976,98	230	1516,50
	12	231	1081,22	253	1036,87	240	1208,48	207	1277,82	182	1483,63	261	1060,06	225	1506,95
	13	350	820,84	466	453,96	369	982,99	245	1510,84	458	428,94	279	1460,25	364	954,27
	14	314	960,78	473	524,21	336	1086,57	253	1359,56	504	494,34	274	1493,69	348	1043,00
	15	268	1198,10	414	647,47	339	1040,95	206	1704,56	436	726,94	256	1601,52	300	1231,92
	16	297	956,00	352	738,38	325	919,00	290	1237,77	403	814,18	328	1153,57	328	1038,30
	17	265	825,21	312	778,32	307	743,51	299	958,59	366	829,79	435	684,58	367	811,75
	18	248	1026,21	265	887,35	281	838,31	238	1388,28	334	934,32	306	964,00	302	1018,02
	19	169	1487,24	265	869,58	247	1096,30	174	1976,20	260	1145,81	212	1448,23	221	1489,35
	20	196	1498,75	246	899,48	206	1292,80	161	2314,71	257	1105,80	209	1548,44	221	1565,90
	21	261	965,72	450	517,95	308	806,62	223	1613,16	458	584,52	336	1063,80	305	1257,32
	22	267	959,07	434	596,50	236	997,43	233	1568,12	417	720,29	353	1016	338	1079,36
	23	243	922,53	396	611,00	226	963,05	229	1490,45	424	636,38	385	831,53	341	879,14
	24	208	886,71	269	827,26	234	792,47	251	111,88	326	684,03	408	664,20	367	694,77
	25	174	1117,84	264	855,35	236	830,12	240	1273,30	269	967,75	212	1147,00	290	1010,85
	26	139	1523,60	462	526,49	235	669,88	239	868,15	379	676,79	338	779,88	296	1335,71
	27	146	1443,94	417	607,12	196	1029,70	228	1316,34	398	753,82	328	795,00	273	1402,21
	28	153	1302,47	330	714,07	163	1197,84	232	1393,98	415	708,54	357	913,95	335	974,68
	29	177	1077,97	287	798,62	171	960,30	237	1046,93	345	799,233	378	710,16	363	796,82
	30	182	1120,54	274	881,78	189	890,86	203	1205,27	285	1066,86	296	957,43	305	1023,81

channels		F3 → P3		Fz → P3		F4 → P3		F3 → P4		Fz → P4		F4 → P4		C4 → C3	
		n.win	avg	n.win	avg	n.win	avg	n.win	avg	n.win	avg	n.win	avg	n.win	avg
freq	1	526	370,42	643	327,22	540	379,97	458	395,5	571	341,35	553	426,48	547	346,17
	2	567	398,80	567	504,03	555	433,63	518	443,28	617	389,01	584	452,33	610	382,61
	3	555	479,36	479	614,70	498	552,73	541	504,16	545	493,28	564	486,79	579	480,14
	4	507	526,72	423	639,31	470	575,63	453	538,86	455	521,76	504	509,37	502	535,06
	8	164	1883,60	165	2058,92	151	2063,35	227	967,51	216	1371,81	123	2912,03		
	9	188	1481,45	194	1632,12	199	1551,32	236	920,00	210	1307,59	162	2114,88	224	1118,69
	10	242	1187,24	209	1469,57	288	939,76	227	1018,44	201	1344,06	232	1267,34	215	1022,09
	11	209	1346,82	213	1516,43	234	1085,49	253	1055,55	248	1230,69	225	1155,11	262	987,26
	12	220	1223,17	206	1591,76	223	1279,44	207	1381,69	235	1346,71	249	1031,95	259	1136,66
	13	117	3685,66	128	3258,36	188	2181,02	438	468,06	370	796,83	368	689,97	395	481,62
	14	102	4279,40	103	4185,06	162	2549,86	432	521,29	385	788,60	400	664,11	426	539,80
	15	94	4615,17	67	6673,25	173	2361,55	366	683,55	394	804,26	385	734,48	452	632,37
	16	164	2488,97	114	3795,62	199	1908,02	351	762,68	421	664,41	365	764,35	448	692,47
	17	225	1378,96	241	1375,65	261	1280,76	355	774,36	384	634,14	344	709,96	369	735,57
	18	235	1338,90	238	1333,89	229	1132,41	300	998,4	270	1150,1	293	956,27	289	915,04
	19	167	1978,53	180	1837,29	140	1805,68	230	1269,13	193	1775,1	197	1696,78	268	951,51
	20	131	2629,08	145	2351,68	135	2035,05	182	1577,13	147	1348,34	190	1770,55	208	1247,68
	21	85	4643,23	59	7354,84	32	14542,0	374	569,31	366	850,32	345	872,27	375	569,85
	22	100	4111,98	41	11169,24	64	7124,26	389	682,20	318	985,68	301	976,58	386	704,21
	23	146	2550,55	184	2144,0	206	1908,19	364	765,67	304	991,86	309	827,81	339	703,49
	24	203	1323,40	223	1249,48	194	1453,05	325	739,90	337	860,46	320	693,60	339	755,12
	25	155	1896,40	162	1902,13	172	1773,02	261	867,93	204	1369,50	242	1049,66	254	1081,64
	26	58	7788,5	117	3162,94	86	5090,03	293	874,98	256	1375,58	225	1522,4	325	606,56
	27	48	9415,31	81	4461,91	111	3835,57	279	946,15	255	1309,70	235	1432,39	372	692,56
	28	139	2788,86	122	3127,31	151	2334,05	284	855,94	259	1049,44	270	1119,45	330	840,08
	29	166	1668,30	169	1837,49	183	1736,53	216	967,98	298	880,12	277	980,29	328	842,98
	30	177	1381,01	176	1711,65	169	1644,92	224	1036,93	215	1339,74	197	1495,72	282	1044,53

Table A.8:

Total samples: 449521

channels		P3 → F3		P3 → Fz		P3 → F4		P4 → F3		P4 → Fz		P4 → F4		C3 → C4	
		n.win	avg	n.win	avg	n.win	avg	n.win	avg	n.win	avg	n.win	avg	n.win	avg
freq	1	545	390.15	630	323.97	565	354.93	504	576.05	578	294.61	445	661.87	691	308.43
	2	604	412.56	642	380.60	568	430.10	462	672.09	588	381.80	511	553.15	652	424.38
	3	538	539.48	553	487.08	521	528.86	466	693.32	523	507.43	557	500.44	575	536.60
	4	466	627.15	523	523.70	473	590.62	506	560.31	466	595.01	525	529.64	535	529.96
	5	244	1537.3	485	591.59	292	1212.4	317	1117.5	479	511.15	373	821.41	417	705.65
	6	271	1343.5	419	664.64	302	1138.6	318	1065.3	409	650.56	375	677.45	411	698.52
	7	318	977.33	373	719.28	326	916.83	341	887.49	361	714.22	370	661.91	388	709.92
	8	59	5633.01	83	4056.46	333	800.85	62	6632.32	67	5781.13	390	611.14	256	1359.8
	9	76	4360.197	38	5303.736	335	859.531	46	9062.673	56	7172.821	385	700.335	232	1602.57
	10	129	2959.07	24	7960.583	372	893.752	31	10434.67	17	24274.82	369	874.411	190	2073.66
	11	332	971.64	23	13371.1	339	949.26	198	1857.5	18	22904.7	350	892.06	326	1105.0
	12	228	1453.19	79	5207.329	264	1232.51	237	1365.16	53	7983.452	162	2298.49	133	2961.18
	13	206	1655.5	170	1240.0	254	1106.9	156	1765.4	74	3544.82	225	929.23	117	3157.0
	14	223	1587.67	162	1448.39	176	2041.60	170	1678.80	87	2149.252	261	1299.42	102	3619.45
	15	228	1598.16	138	1867.78	107	3773.13	207	1448.50	42	4788.64	164	2252.76	133	3040.92
	16	231	1448.83	109	2997.06	83	4868.66	237	1303.68	53	3822.415	177	1649.18	222	1600.5
	17	278	1028.6	143	2076.8	123	3137.1	328	857.88	99	3844.35	165	1837.0	352	832.62
	18	224	1516.77	222	1228.86	108	3501.80	262	1008.35	229	1458.62	125	2979.61	192	1799.02
	19	80	4847.36	220	1163.93	64	6159.953	184	1690.74	195	1787.69	91	4374.25	113	3420.66
	20	35	12016.1	243	1231.7	40	9981.25	142	2334.5	124	2447.0	91	4376.17	74	5476.17
	21	176	1782.0	222	1065.3	302	835.36	215	1275.6	245	1277.3	147	2705.4	46	7516.17
	22	96	3590.15	176	1840.67	165	2077.30	257	1207.77	249	1340.54	88	4498.23	42	10341.71
	23	148	2583.78	201	1812.85	165	2028.92	281	1218.36	254	1332.64	174	2000.70	149	2733.67
	24	295	940.925	248	1227.43	153	2040.14	281	1049.37	285	1068.72	122	2745.83	304	1038.87
	25	206	1569.8	243	1097.5	151	2332.9	232	1330.7	304	954.46	82	4803.57	221	1491.1
	26	203	1731.69	281	1193.00	261	1108.70	182	1765.55	335	900.062	218	1427.36	158	2475.62
	27	164	2346.95	235	1563.69	192	1689.97	200	1817.32	279	1197.81	166	2077.05	172	2369.98
	28	206	1641.23	210	1719.42	153	2087.69	242	1442.08	265	1308.04	157	2071.75	295	1201.06
	29	240	1198.9	241	1342.9	164	2017.7	336	831.80	245	1368.9	136	2444.4	322	791.84
	30	142	2638.19	275	1133.12	127	2879.45	275	1052.85	265	1221.10	142	2561.36	217	1423.45

channels		F3 → P3		Fz → P3		F4 → P3		F3 → P4		Fz → P4		F4 → P4		C4 → C3	
		n.win	avg	n.win	avg	n.win	avg	n.win	avg	n.win	avg	n.win	avg	n.win	avg
freq	1	525	436.21	491	385.54	481	494.09	574	341.25	570	398.32	517	555.35	636	303.90
	2	568	459.87	549	403.69	508	518.85	589	406.01	592	429.29	533	554.71	614	374.79
	3	521	541.21	539	479.00	481	627.02	569	488.86	542	514.81	541	558.15	561	470.64
	4	443	564.07	512	492.31	509	595.78	516	537.94	525	548.22	542	514.78	518	520.73
	5	414	670.94	472	596.34	392	705.00	326	999.16	486	580.26	336	1058.00	536	445.12
	6	404	653.45	465	577.59	363	794.01	323	949.62	435	637.01	389	809.85	491	523.83
	7	390	663.84	420	608.31	361	736.18	332	828.67	444	599.97	348	782.78	462	606.10
	8	547	397.93	500	417.25	410	415.20	110	3796.4	163	2536.2	187	2138.0	409	726.60
	9	457	692.157	472	614.921	443	521.801	107	3950.01	171	2383.30	193	2084.00	325	1108.56
	10	367	919.20	434	760.79	387	763.97	147	2809.5	200	1986.2	234	1686.2	237	1638.8
	11	313	1012.4	321	923.73	335	899.47	251	1447.1	345	941.23	318	981.41	276	1290.0
	12	219	1542.07	257	1249.28	304	1043.54	94	4340.957	135	3002.28	100	4174.50	216	1575.85
	13	472	415.22	437	448.37	489	369.79	93	4597.81	100	4257.98	59	7378.10	275	1033.79
	14	465	529.54	445	585.05	480	509.66	82	5235.84	99	4247.20	76	5675.92	273	1128.37
	15	377	822.32	352	857.63	368	772.76	126	3320.33	129	3181.62	143	2877.40	292	1164.37
	16	300	1090.28	299	1034.58	324	870.02	244	1456.84	269	1346.21	288	1120.07	265	1203.83
	17	301	1127.8	286	1134.0	275	1096.8	322	898.13	312	929.06	328	795.77	296	981.01
	18	199	1707.65	229	1402.58	242	1326.72	163	2185.06	186	1886.04	169	2013.19	278	1105.10
	19	194	1680.72	256	1155.30	238	1373.76	93	4197.02	85	4534.87	92	4437.76	238	1178.32
	20	194	1625.7	265	999.55	234	1256.0	78	5189.35	69	5785.18	59	7212.35	188	1379.9
	21	319	948.25	318	761.69	335	590.68	63	6620.93	99	4241.37	63	6839.26	290	1128.75
	22	275	1206.91	330	857.842	362	669.541	113	3659.25	144	2826.60	113	3677.89	266	1229.76
	23	319	1037.3	349	842.20	305	855.71	266	1323.1	303	1122.5	321	1055.5	310	954.60
	24	313	860.43	340	836.57	277	1052.0	305	860.49	335	820.26	335	767.49	319	898.18
	25	266	1000.87	265	1109.14	253	1269.47	196	1554.22	195	1693.32	222	1486.26	266	1056.27
	26	236	1407.0	278	1088.8	286	800.37	191	1981.6	129	2939.2	118	3352.8	297	759.00
	27	207	1669.6	298	1088.4	291	955.65	206	1842.8	208	1879.1	173	2297.7	341	720.42
	28	212	1599.0	304	1105.8	314	997.78	305	1001.0	255	1370.9	297	1114.8	351	795.79
	29	289	1026.6	342	885.97	321	924.14	299	832.99	272	1067.1	309	898.16	343	825.20
	30	267	1130.38	295	994.138	246	1115.58	240	1321.72	185	1794.90	189	1747.72	260	1000.41

Table A.9:

Total samples: 200484

channels		P3 → F3		P3 → Fz		P3 → F4		P4 → F3		P4 → Fz		P4 → F4		C3 → C4	
		n.win	avg	n.win	avg	n.win	avg	n.win	avg	n.win	avg	n.win	avg	n.win	avg
freq	13	137	1008.5	135	757.86	106	1579.7	160	1002.3	163	579.81	127	1244.4	142	839.16
	14	142	1098.3	159	700.11	92	1895.77	145	1164.2	149	693.73	120	1346.5	134	953.65
	15	150	1074.6	177	712.08	72	2437.36	119	1472.7	158	740.72	121	1334.4	153	981.64
	16	140	1085.5	172	681.00	94	1772.37	137	1185.0	176	767.93	146	990.04	174	871.16
	17	186	771.01	143	782.79	138	1036.9	168	859.26	182	711.55	162	780.12	145	892.79
	18	133	1022.81	127	980.669	129	1025.27	121	1209.75	138	889.463	119	1095.18	124	1083.42
	19	92	1474.53	103	1248.00	106	1189.13	89	1610.78	110	1063.69	110	1356.45	108	1206.18
	20	77	1845.41	108	1225.70	107	1192.66	89	1680.49	125	985.61	94	1680.45	114	1147.07
	25	87	2041.88	148	549.75	127	1135.3	133	1117.9	233	372.21	85	1875.34	166	760.36
	26	83	2159.65	163	543.30	119	1264.8	137	1128.5	250	409.42	84	1916.13	166	801.82
	27	95	1851.41	194	536.15	108	1426.7	111	1468.1	220	600.32	98	1770.84	172	786.09
	28	121	1340.6	184	613.72	121	1204.8	114	1378.3	195	707.37	127	1297.5	139	832.01
	29	161	823.83	148	986.44	148	893.26	145	960.43	172	724.51	171	792.65	145	715.53
	30	107	1355.4	133	986.64	119	1157.1	109	1166.6	128	872.57	140	950.80	132	919.65

channels		F3 → P3		Fz → P3		F4 → P3		F3 → P4		Fz → P4		F4 → P4		C4 → C3	
		n.win	avg	n.win	avg	n.win	avg	n.win	avg	n.win	avg	n.win	avg	n.win	avg
freq	13	130	1250.7	125	1219.9	158	904.98	199	427.83	167	532.89	205	412.53	181	482.89
	14	122	1355.3	135	1161.1	153	982.73	207	495.47	155	625.52	206	455.79	190	518.00
	15	136	1208.1	126	1277.8	175	853.02	186	694.57	171	645.52	181	595.92	179	664.02
	16	151	968.60	147	1044.4	158	833.02	172	787.22	185	656.93	174	639.77	192	704.77
	17	163	852.95	170	772.81	149	855.56	150	898.54	188	648.53	164	654.45	185	683.81
	18	157	843.23	125	1128.8	160	853.01	109	1378.3	158	822.18	151	758.24	158	759.11
	19	122	1090.9	76	1946.93	124	1111.9	91	1671.87	134	1025.8	150	827.34	131	907.82
	20	117	1188.8	88	1660.72	83	1489.02	91	1616.72	131	1060.0	151	766.76	137	904.58
	25	59	3009.27	105	1523.1	101	1659.3	193	422.25	186	493.12	227	421.68	179	507.81
	26	54	3350.46	102	1577.5	85	2041.50	185	510.53	194	508.39	208	581.08	201	512.62
	27	79	2175.93	106	1506.4	80	2209.91	185	584.29	170	658.34	193	732.35	190	609.77
	28	138	992.73	121	1301.7	143	990.81	157	621.23	174	747.77	176	832.50	165	730.65
	29	144	783.36	134	1101.0	123	621.73	143	729.37	158	838.33	154	966.22	131	810.41
	30	103	1222.5	126	1077.0	121	869.41	105	1183.6	127	850.19	135	1016.0	116	863.56

Table A.10:

Total samples: 484030

channels		P3 → F3		P3 → Fz		P3 → F4		P4 → F3		P4 → Fz		P4 → F4		C3 → C4	
		n.win	avg	n.win	avg	n.win	avg	n.win	avg	n.win	avg	n.win	avg	n.win	avg
freq	8	545	431,33	400	373,92	555	437,06	593	484,77	710	323,82	522	566,80	540	538,57
	9	458	744,42	499	399,69	420	787,19	372	1060,55	614	516,77	315	1322,60	349	1128,65
	10	380	993,82	513	519,43	340	1061,56	276	1518,41	576	592,75	232	1792,01	272	1510,72
	11	388	813,51	413	659,29	389	851,84	346	1088,71	517	570,21	294	1275,54	295	1232,04
	12	344	801,21	385	658,91	314	1005,84	315	1108,33	370	827,05	276	1278,69	253	1390,27
	13	433	814,44	517	425,82	495	649,68	378	992,82	531	461,80	456	791,90	480	537,40
	14	368	1003,50	513	517,34	444	788,87	321	1236,80	514	537,35	418	884,21	516	579,24
	15	346	1107,26	475	630,31	401	919,97	297	1395,81	518	580,91	422	868,93	468	736,99
	16	391	925,90	491	616,62	395	889,23	352	1085,57	450	663,22	407	817,04	412	801,10
	17	420	721,86	397	726,69	421	739,77	349	868,15	409	691,06	414	693,38	386	777,18
	18	355	848,83	332	845,74	313	898,53	349	932,34	353	823,30	279	1073,71	321	961,18
	19	264	1220,39	286	970,91	267	1097,71	238	1433,57	314	967,60	211	1686,35	278	1092,82
	20	217	1647,72	275	1061,21	243	1355,23	224	1467,32	304	1014,10	171	2332,89	272	1170,01
	21	418	882,91	503	603,74	401	797,82	318	1274,29	494	544,36	471	661,68	471	646,58
	22	345	1107,82	446	752,89	364	905,58	313	1281,07	506	597,11	436	729,15	468	694,87
	23	370	917,66	411	768,91	381	840,09	359	989,12	454	663,01	431	712,07	446	664,92
	24	315	905,68	392	737,79	376	822,09	342	902,01	360	857,02	380	777,92	401	736,18
	25	300	1062,76	327	940,21	282	1053,78	283	1067,61	249	1368,60	290	1203,59	320	977,84
	26	292	1297,95	560	530,66	437	766,05	238	1755,36	555	545,86	379	896,97	402	827,39
	27	237	1742,98	467	728,75	394	926,31	215	1979,88	513	635,34	381	935,62	366	1002,46
	28	283	1355,26	390	868,40	385	862,12	314	1199,01	435	720,13	396	832,64	343	1018,20
	29	342	921,22	365	875,89	372	779,28	344	858,37	386	736,29	387	814,77	355	819,91
	30	286	1187,56	324	941,09	317	937,36	285	1153,27	300	934,52	265	1221,43	339	830,23

channels		F3 → P3		Fz → P3		F4 → P3		F3 → P4		Fz → P4		F4 → P4		C4 → C3	
		n.win	avg	n.win	avg	n.win	avg	n.win	avg	n.win	avg	n.win	avg	n.win	avg
	8	78	5792,73	105	4335,70	184	2285,73	517	515,22	544	513,30	544	453,55	697	309,04
	9	11	35922,90	31	12506,22	32	12385,15	405	934,91	388	1007,93	420	854,60	680	405,66
	10	12	23843,25	45	8614,82	18	22127,83	320	1279,58	286	1472,50	348	1132,05	550	577,88
	11	31	11645,77	90	4155,48	97	3830,70	353	1038,35	366	980,67	381	957,74	476	670,44
	12	15	24577,8	48	8134,33	35	9851,54	265	1309,97	297	1103,47	268	1235,71	372	802,50
	13	426	775,01	413	850,79	463	720,19	489	688,65	425	783,73	437	760,79	588	411,89
	14	414	865,0	364	1024,24	416	849,75	442	805,62	397	879,85	401	864,58	640	434,20
	15	352	1081,72	357	1080,03	397	924,30	429	841,36	355	1011,49	404	898,41	563	580,09
	16	350	1009,35	389	916,23	382	886,79	430	797,64	377	912,08	407	867,78	495	674,67
	17	396	781,79	383	796,92	401	785,53	410	682,43	377	793,98	402	777,37	414	795,11
freq	18	337	945,37	330	970,19	289	1154,66	337	864,36	312	926,30	310	1031,29	341	933,25
	19	215	1575,85	234	1403,15	233	1409,52	275	1072,99	255	1212,94	199	1680,17	282	1039,38
	20	195	1921,83	186	1919,13	200	1722,26	221	1362,66	232	1369,94	186	1946,45	239	1158,51
	21	391	863,94	378	919,89	406	837,89	432	776,36	376	859,95	475	644,46	530	520,55
	22	321	1154,55	337	1074,29	324	1102,67	400	875,04	357	965,46	453	718,10	447	692,29
	23	320	1091,67	337	976,94	357	920,81	385	890,82	384	888,83	425	764,10	475	646,64
	24	306	1000,76	399	695,40	364	849,04	393	849,05	388	822,35	369	765,41	383	833,04
	25	261	1246,02	312	998,14	277	1086,80	335	932,86	299	998,84	295	1030,04	301	1055,73
	26	401	819,00	404	813,94	407	844,91	374	975,48	414	780,20	354	971,07	480	587,84
	27	365	992,35	347	1025,95	347	1076,51	361	1074,16	394	880,42	331	1106,33	448	698,51
	28	350	978,32	335	1020,64	366	928,88	380	924,60	406	791,39	406	845,45	445	634,85
	29	308	996,92	342	945,40	387	732,58	371	803,18	354	808,82	368	822,08	330	776,82
	30	308	969,46	342	926,39	345	814,16	294	1050,40	292	1018,96	294	1077,07	283	917,36

Table A.11:

Total samples: 453310

channels		P3 → F3		P3 → Fz		P3 → F4		P4 → F3		P4 → Fz		P4 → F4		C3 → C4	
		n.win	avg	n.win	avg	n.win	avg	n.win	avg	n.win	avg	n.win	avg	n.win	avg
	3	488	471,43	511	342,58	298	1246,90	353	930,81	629	314,68	586	530,08	501	446,25
	4	386	841,41	566	390,98	288	1304,70	345	991,08	594	417,18	300	1296,57	508	503,24
	5	282	1277,34	508	548,48	288	1291,63	343	1017,58	504	548,39	218	1780,46	447	618,11
	6	310	1148,98	461	630,69	343	981,66	344	944,42	446	612,55	235	1565,77	432	582,62
freq	7	309	1034,33	433	638,61	423	684,00	382	726,26	378	761,86	238	1440,69	398	590,81
	8	384	861,86	509	455,48	348	910,24	368	906,84	515	445,02	407	713,38	471	434,23
	9	128	3261,02	510	526,52	237	1638,24	187	2109,47	491	550,13	212	1901,20	560	470,85
	10	91	4708,10	429	687,45	194	2094,66	108	3740,45	407	760,80	143	2873,61	480	697,47
	11	94	4272,10	407	673,31	273	1343,41	198	1970,43	401	739,64	214	1723,71	382	723,98
	12	146	2648,83	360	712,2	273	1152,36	216	1600,03	347	801,39	234	1415,44	306	863,39

channels		F3 → P3		Fz → P3		F4 → P3		F3 → P4		Fz → P4		F4 → P4		C4 → C3	
		n.win	avg	n.win	avg	n.win	avg	n.win	avg	n.win	avg	n.win	avg	n.win	avg
freq	3	459	645,15	448	712,01	263	1448,56	288	1251,01	416	747,02	402	879,60	515	394,75
	4	372	941,18	361	1019,86	240	1634,37	269	1369,10	332	1100,73	235	1713,54	552	449,89
	5	285	1320,64	274	1449,00	240	1604,62	306	1188,13	257	1517,64	177	2320,83	508	588,71
	6	335	1011,28	295	1247,28	305	1118,80	367	851,60	258	1394,75	241	1530,96	450	686,12
	7	307	953,84	304	1087,57	334	853,60	364	692,14	288	1102,39	263	1160,06	408	730,14
	8	384	929,75	421	803,56	332	1106,46	310	1230,68	301	1269,54	319	1232,70	653	350,00
	9	99	4390,14	167	2521,53	126	3331,58	81	5053,51	68	6007,91	41	10080,17	553	536,98
	10	64	6663,992	123	3489,32	105	4032,63	84	4877,65	49	7690,61	42	9902,83	461	716,21
	11	134	3023,20	206	1906,50	210	1854,19	161	2537,40	125	3344,15	89	4846,93	415	715,54
	12	108	3642,52	154	2528,32	156	2479,48	90	4738,66	93	4508,87	28	15925,46	373	737,87

Table A.12:

Total samples: 498366

channels		P3 → F3		P3 → Fz		P3 → F4		P4 → F3		P4 → Fz		P4 → F4		C3 → C4	
		n.win	avg	n.win	avg	n.win	avg	n.win	avg	n.win	avg	n.win	avg	n.win	avg
freq	1	523	489,18	603	352,05	540	469,32	519	546,24	639	326,87	537	499,82	641	327,04
	2	571	517,97	675	405,43	518	568,14	527	567,95	657	411,60	553	569,90	609	425,26
	3	501	605,32	532	594,14	463	662,17	548	558,85	588	512,19	481	667,61	528	562,60
	4	449	526,16	455	669,05	438	631,01	556	530,57	526	564,32	413	689,12	458	679,94
	5	377	916,25	485	583,51	324	1024,58	351	1043,57	440	739,41	364	946,82	542	524,09
	6	319	998,16	458	642,21	322	998,19	367	952,67	437	741,62	327	983,86	463	644,41
	7	299	1000,53	382	764,62	335	908,75	407	760,99	401	792,03	326	943,16	420	735,07
	8	410	934,25	583	361,38	202	2250,11	328	1227,03	663	328,19	253	1635,64	465	473,38
	9	175	2657,26	602	463,21	71	5962,84	106	4402,37	700	406,22	158	2850,61	549	542,89
	10	199	2253,45	539	599,68	84	5623,82	93	5070,70	572	574,22	132	3469,31	442	870,66
	11	242	1556,71	448	634,72	251	1663,79	212	2077,61	410	729,18	233	1788,51	431	869,45
	12	147	3145,78	386	793,75	225	1741,37	219	1780,77	299	1026,85	125	3541,84	410	802,53
	13	144	3263,87	404	532,80	195	1326,05	223	1925,33	495	550,92	99	3383,29	378	682,35
	14	162	2884,49	436	588,05	166	1606,70	190	2330,5	433	726,57	98	3452,37	403	683,25
	15	161	2816,80	419	754,41	183	1887,73	150	3027,69	403	860,16	103	3282,09	429	701,65
	16	250	1595,32	362	919,47	215	1724,44	200	2162,43	362	882,44	203	2086,82	403	756,93
	17	364	863,07	329	922,92	276	1239,41	332	994,75	352	772,07	327	972,59	400	705,22
	18	238	1596,77	314	937,19	287	1163,40	280	1247,12	313	871,91	225	1656,16	324	961,97
	19	130	3249,55	291	980,21	217	1554,21	185	2122,59	297	1036,26	137	3013,27	270	1217,09
	20	116	3819,09	316	869,58	161	2300,71	145	2789,24	322	977,31	97	4629,05	258	1295,44
	21	184	2212,24	495	595,83	278	798,89	198	1766,47	517	609,83	134	2252,91	377	890,57
	22	212	1833,13	380	942,76	221	1158,72	223	1557,07	391	934,47	152	1915,65	431	778,32
	23	326	1075,06	357	975,03	252	1590,86	314	1032,36	344	1009,05	238	1674,11	431	689,48
	24	320	926,13	361	827,26	322	873,07	315	943,27	325	988,03	323	989,45	412	680,05
	25	202	1821,85	315	936,74	230	1189,48	234	1527,43	274	1287,60	193	1742,69	276	1104,53
	26	138	3013,23	480	707,23	177	1549,14	185	1946,62	356	898,39	79	4092,97	306	1020,44
	27	184	2165,14	442	790,87	193	1416,57	207	1687,07	346	905,30	111	3533,76	291	1137,87
	28	240	1565,62	407	668,01	235	1409,48	261	1300,59	312	876,86	278	1204,06	350	880,61
	29	296	1065,85	415	715,57	306	952,66	325	970,0	375	785,77	294	873,25	360	732,47
	30	198	1902,22	303	1085,23	229	1214,89	270	1164,3	315	1140,30	210	1289,74	262	1051,32

channels		F3 → P3		Fz → P3		F4 → P3		F3 → P4		Fz → P4		F4 → P4		C4 → C3	
		n.win	avg	n.win	avg	n.win	avg	n.win	avg	n.win	avg	n.win	avg	n.win	avg
freq	1	681	359,51	551	475,33	500	501,55	491	584,81	512	485,80	564	397,37	662	352,78
	2	578	576,93	592	468,90	474	616,20	482	633,05	539	502,61	551	558,95	696	411,11
	3	445	747,08	596	486,27	468	670,84	483	653,32	472	602,34	436	764,68	596	528,01
	4	391	752,57	524	497,49	506	599,98	455	630,20	441	613,97	412	749,80	502	593,15
	5	392	749,28	466	545,87	354	885,74	265	1562,27	463	692,29	401	872,44	512	661,25
	6	317	847,04	400	606,59	382	782,01	286	1308,12	423	737,17	337	1030,83	448	736,20
	7	288	845,21	361	629,08	350	791,23	331	961,57	423	654,39	319	986,67	430	702,36
	8	482	477,78	431	524,33	423	562,89	446	712,55	413	769,49	429	731,95	390	679,85
	9	444	680,93	543	535,53	390	778,71	272	1555,37	336	1205,68	375	1040,21	407	810,64
	10	355	1011,85	411	922,81	357	1000,43	240	1795,35	303	1445,90	328	1221,83	349	1107,26
	11	337	1030,67	443	851,41	417	826,90	267	1541,82	248	1649,15	291	1265,96	377	957,93
	12	284	1300,17	275	1449,30	340	890,50	189	2287,16	148	2974,82	134	3378,90	384	829,49
	13	478	564,89	380	750,59	338	799,10	377	782,22	314	982,0	319	967,02	311	707,15
	14	488	609,32	359	830,13	377	793,00	398	835,79	331	982,56	312	1012,35	320	759,99
	15	493	672,52	386	841,08	384	869,22	351	1047,46	281	1234,63	310	1032,41	359	797,39
	16	437	710,37	380	874,01	391	860,56	328	1117,18	309	1118,12	364	853,93	363	860,99
	17	377	781,24	384	867,53	354	947,92	321	995,72	346	1039,72	337	1011,84	371	773,39
	18	293	1039,19	256	1333,86	294	1171,21	323	955,34	259	1206,26	254	1246,67	270	1087,95
	19	224	1201,73	231	1530,19	263	1350,95	274	1174,81	209	1475,88	178	1832,54	239	1253,26
	20	223	1177,52	220	1580,34	227	1580,19	241	1355,88	199	1673,08	166	2084,86	220	1358,68
	21	406	852,58	425	771,64	418	808,52	298	1090,99	339	1097,77	259	1508,97	231	935,90
	22	319	1175,63	413	854,59	433	816,78	302	1218,85	370	997,72	235	1657,65	286	803,34
	23	321	1081,40	356	979,01	340	936,49	304	1136,02	359	922,29	335	1010,20	362	849,27
	24	328	974,64	343	977,20	303	1025,48	326	832,91	395	722,33	303	1048,38	364	855,82
	25	251	1381,77	260	1300,66	241	1377,51	301	837,20	227	1332,09	243	1347,58	268	1145,39
	26	379	846,08	340	937,91	438	708,31	351	922,71	315	1056,66	275	1307,44	263	889,94
	27	348	967,99	322	1021,02	373	874,32	318	1136,26	283	1320,46	241	1518,98	324	829,30
	28	384	777,88	318	997,08	350	786,41	322	1090,53	325	1142,38	256	1157,14	397	864,22
	29	318	834,01	311	1004,15	327	717,24	334	872,85	338	983,90	204	1160,58	370	799,3
	30	268	1196,62	296	1094,47	265	932,37	274	1034,44	272	1294,87	237	1243,48	238	1242,81

Table A.13:

Total samples: 436107

channels		P3 → F3		P3 → Fz		P3 → F4		P4 → F3		P4 → Fz		P4 → F4		C3 → C4	
		n.win	avg	n.win	avg	n.win	avg	n.win	avg	n.win	avg	n.win	avg	n.win	avg
freq	1	468	556,98	444	506,14	603	351,24	96	4059,27	715	306,51	589	422,02	707	303,64
	2	348	982,56	483	529,15	652	413,58	214	1815,74	542	561,71	638	413,69	635	454,39
	3	232	1545,79	462	654,12	537	561,41	300	1060,26	433	727,55	580	508,91	501	615,14
	4	290	1108,50	453	666,78	537	565,16	330	949,10	450	666,23	445	671,69	424	643,45
	5	277	1271,07	235	1496,42	390	695,2	270	1234,89	466	636,36	422	746,20	451	698,74
	6	298	1114,73	256	1376,46	366	755,87	362	859,85	432	656,14	443	653,08	414	748,56
	7	286	1049,35	321	976,39	357	740,38	428	596,67	391	659,80	438	600,11	353	840,19
	8	317	863,38	508	392,64	411	634,05	260	1378,05	626	319,34	418	662,07	454	511,93
	9	274	1249,89	492	496,44	228	1614,87	114	3542,83	563	466,61	267	1371,88	381	865,68
	10	182	2104,53	454	656,63	164	2338,68	100	3880,75	515	591,83	182	2113,77	295	1244,52
	11	252	1357,38	363	706,53	211	1725,05	156	2448,75	399	726,38	201	1839,76	291	1192,74
	12	234	1417,28	310	760,58	178	2012,15	147	2606,56	348	810,40	166	2293,83	264	1276,10
	13	299	1161,19	521	403,84	426	617,78	294	1195,38	495	348,53	266	1287,26	391	845,61
	14	273	1311,34	532	459,20	390	794,06	273	1330,25	522	405,30	245	1421,44	333	1060,92
	15	230	1586,06	480	573,04	357	935,79	246	1487,68	480	523,56	258	1352,25	315	1153,44
	16	235	1440,69	380	741,08	326	944,64	288	1173,30	407	639,76	307	1018,24	334	1007,95
	17	326	914,31	334	809,41	365	750,04	321	911,85	350	737,15	334	808,97	353	817,14
	18	274	1016,76	283	966,70	281	995,88	263	1052,37	346	816,78	282	1035,81	288	999,38
	19	216	1254,04	232	1256,61	202	1338,72	171	1567,32	279	1037,09	175	1701,76	208	1394,90
	20	203	1334,29	239	1236,34	209	1225,23	188	1536,07	250	1121,97	154	2057,94	199	1598,46
	21	216	1627,38	389	494,28	370	746,84	241	1538,95	578	378,70	242	1552,90	176	2172,67
	22	196	1813,70	369	618,33	321	1037,77	196	1894,42	481	560,24	232	1621,61	146	2646,72
	23	270	1223,63	313	751,10	334	919,83	272	1202,95	396	718,14	283	1178,00	244	1538,45
	24	308	885,50	283	871,76	302	904,82	331	804,57	312	913,52	367	790,57	332	934,36
	25	258	1143,87	237	1148,64	225	1302,85	231	1284,52	276	1048,27	273	983,99	253	1205,24
	26	158	2393,27	430	513,83	268	1015,15	184	2019,60	450	577,07	183	1939,43	103	3796,83
	27	129	3019,10	407	651,74	224	1422,71	205	1756,05	382	786,56	132	2776,53	98	4097,16
	28	167	2219,38	341	805,60	270	1275,38	299	1016,41	370	7 84,89	204	1773,86	206	1761,72
	29	263	1141,88	321	828,10	306	1008,72	323	797,61	333	774,04	288	987,60	334	832,67
	30	246	1133,80	292	898,55	245	1236,50	226	1342,62	279	869,87	270	992,60	250	1191,62

channels		F3 → P3		Fz → P3		F4 → P3		F3 → P4		Fz → P4		F4 → P4		C4 → C3	
		n.win	avg	n.win	avg	n.win	avg	n.win	avg	n.win	avg	n.win	avg	n.win	avg
freq	1	709	364,68	356	878,83	342	1009,51	503	577,15	728	310,54	473	528,88	454	397,99
	2	375	961,58	383	852,02	371	909,89	485	631,03	565	529,34	472	578,97	532	391,77
	3	339	1026,15	387	807,06	420	738,63	530	566,25	457	658,97	484	637,46	540	461,72
	4	389	674,95	449	655,79	437	575,26	497	470,81	421	678,36	535	521,26	482	546,75
	5	303	1090,63	393	789,97	216	1754,02	335	991,25	271	1348,30	530	480,62	571	514,29
	6	266	1147,04	366	834,79	240	1572,89	353	861,98	273	1268,13	437	563,28	459	585,73
	7	294	908,53	395	721,73	312	1004,96	380	724,66	298	1035,30	408	581,84	353	726,88
	8	340	818,46	397	780,30	398	765,26	473	576,04	518	500,11	435	627,94	553	366,82
	9	339	960,70	348	949,95	329	1068,90	333	1064,85	357	992,56	240	1578,02	509	531,80
	10	284	1275,17	316	1125,92	299	1218,94	261	1453,33	259	1480,18	184	2173,94	455	682,10
	11	307	951,30	403	773,87	368	827,16	289	11149,99	281	1197,83	261	1343,85	353	789,40
	12	240	1221,37	297	1018,57	250	1237,55	253	1331,07	225	1493,67	168	2164,21	262	1033,40
	13	268	1067,88	318	948,56	294	1094,45	366	863,99	340	885,56	349	916,42	457	502,08
	14	289	1051,71	311	998,09	316	991,66	345	964,81	307	1051,81	324	1045,54	431	602,56
	15	279	1194,69	288	1132,81	332	963,64	281	1202,19	319	1074,57	297	1187,80	448	644,32
	16	323	1007,06	313	1007,54	382	778,85	300	1065,96	353	915,61	284	1182,53	400	690,25
	17	278	989,90	330	856,96	354	801,94	326	849,84	351	778,22	353	800,45	383	693,94
	18	229	1325,20	257	1155,84	238	1070,44	306	967,04	309	840,26	321	910,59	286	986,23
	19	156	2109,66	181	1706,41	194	1376,94	226	1314,26	234	1221,04	206	1460,86	251	1138,49
	20	154	2146,35	172	1875,74	150	1938,14	146	2227,54	187	1707,35	155	2056,36	202	1364,75
	21	258	1238,51	281	1247,92	325	926,40	273	1288,65	279	1249,75	245	1369,96	424	580,45
	22	259	1313,20	272	1302,32	364	836,16	277	1253,44	272	1304,96	252	1344,34	429	642,37
	23	280	1219,84	329	999,16	398	718,29	318	970,27	343	929,21	301	1021,99	429	640,48
	24	312	893,67	373	718,52	345	829,71	324	859,15	370	734,28	312	851,28	390	653,62
	25	253	1021,37	265	913,33	258	1117,41	239	1219,80	270	1141,34	277	1013,80	311	856,36
	26	342	718,60	266	1289,57	332	984,87	213	1622,15	239	1500,56	287	1117,22	361	650,66
	27	321	910,95	271	1311,38	291	1176,74	231	1473,48	209	1764,59	248	1354,21	374	707,94
	28	322	945,84	292	1133,48	349	898,67	284	1038,45	297	1150,86	326	967,74	390	689,92
	29	358	795,52	341	829,77	360	759,30	315	900,81	266	1129,34	346	838,60	321	851,03
	30	303	906,22	275	1057,99	288	929,17	192	1834,27	259	1215,71	307	960,97	267	1045,59

Table A.14:

Total samples: 487819

channels		P3 → F3		P3 → Fz		P3 → F4		P4 → F3		P4 → Fz		P4 → F4		C3 → C4	
		n.win	avg	n.win	avg	n.win	avg	n.win	avg	n.win	avg	n.win	avg	n.win	avg
	1	573	424,13	618	301,38	495	458,17	576	437,26	695	289,32	618	464,35	554	387,05
	2	580	480,78	634	384,99	483	543,55	589	478,42	682	368,98	594	530,64	576	443,80
	3	570	551,10	612	483,93	512	597,25	587	531,02	530	506,63	540	603,58	532	556,89
	4	553	511,50	533	563,58	537	522,89	574	498,08	530	506,63	462	703,31	4486	629,14
	5	374	1029,08	544	549,89	333	1094,32	354	1075,20	550	522,24	301	1296,17	407	903,73
	6	479	708,96	460	606,28	294	1227,45	373	934,91	499	545,39	446	749,86	391	868,66
	7	437	656,11	408	651,67	333	997,45	376	808,94	442	605,63	426	706,97	365	916,57
	8	507	589,70	591	409,05	370	964,37	537	551,06	561	434,19	346	1005,14	464	708,89
	9	416	931,42	473	712,84	155	2847,00	316	1293,08	489	707,49	229	1851,14	198	2241,67
	10	330	1264,32	405	924,46	105	4193,70	241	1781,54	331	1190,44	167	2707,79	115	4046,94
	11	330	1179,91	393	822,77	164	2570,17	307	1256,84	352	1016,69	187	2304,29	181	2370,66
freq	12	161	2740,98	307	977,81	161	2533,07	272	1329,40	291	1112,32	108	4219,51	170	2405,37
	20	292	1367,36	486	548,56	334	1205,99	335	1148,63	488	550,57	294	1365,23	388	947,89
	21	281	1456,53	483	608,74	277	1499,25	295	1381,78	449	661,54	278	1452,19	322	1231,63
	22	276	1500,78	507	635,83	276	1490,01	286	1462,99	442	744,35	272	1486,41	248	1661,04
	23	388	912,75	425	756,52	350	1018,36	349	1068,38	439	745,66	340	1077,54	278	1416,52
	24	388	727,32	403	813,12	336	831,63	367	828,92	375	800,34	382	797,41	363	910,64
	25	256	1245,06	302	1092,76	295	1030,08	325	942,03	283	1049,89	258	1316,70	283	1002,46
	26	236	1733,37	449	577,72	235	1813,35	288	1407,27	484	614,21	225	1838,64	271	1310,78
	27	239	1717,33	478	623,43	171	2554,07	269	1522,97	437	780,59	236	1746,61	258	1424,59
	28	288	1323,24	415	721,76	253	1588,96	273	1353,15	431	757,85	280	1366,01	295	1263,97
	29	358	846,58	338	828,82	330	1012,50	305	966,48	425	696,50	365	885,96	343	920,38
	30	256	1263,41	303	953,46	286	1202,13	258	1048,89	307	943,18	291	1184,84	310	938,45

channels		F3 → P3		Fz → P3		F4 → P3		F3 → P4		Fz → P4		F4 → P4		C4 → C3	
		n.win	avg	n.win	avg	n.win	avg	n.win	avg	n.win	avg	n.win	avg	n.win	avg
	1	552	528,49	667	372,49	670	361,92	529	388,24	543	361,92	538	465,00	672	331,13
	2	551	571,70	626	489,74	620	483,27	565	440,10	556	453,76	538	505,46	671	408,28
	3	522	657,98	588	581,20	572	570,22	532	577,45	539	556,82	562	555,16	615	506,32
	4	530	566,46	563	553,17	537	601,79	530	615,17	491	644,48	513	611,05	576	517,39
	5	376	967,51	476	646,01	395	838,71	418	843,25	415	764,55	428	842,75	503	656,38
	6	421	738,35	421	711,35	362	860,92	410	827,87	453	647,81	456	642,03	441	680,65
	7	421	687,46	414	685,07	382	664,79	395	759,71	390	770,64	425	696,00	401	727,08
	8	500	510,43	552	510,34	490	515,61	539	416,25	519	415,69	575	442,43	589	511,00
	9	442	829,18	386	1003,84	417	800,04	474	723,97	520	612,45	466	707,57	364	1121,85
	10	317	1323,21	306	1340,97	352	1002,44	314	1273,67	382	990,32	426	840,61	274	1539,03
	11	319	1159,56	323	1089,96	297	960,77	328	1063,14	383	814,97	396	819,08	326	1077,51
freq	12	226	1683,01	304	1100,21	275	1043,26	324	980,20	291	948,22	326	914,72	295	1163,06
	20	459	602,50	506	490,95	487	519,55	521	400,06	463	441,74	474	450,35	445	704,10
	21	445	665,18	499	542,63	484	589,18	544	456,43	493	463,27	541	450,70	382	905,70
	22	426	741,34	488	600,68	438	738,31	569	500,92	499	555,89	510	567,27	365	1001,18
	23	425	716,71	435	670,54	421	820,46	456	626,10	432	713,30	475	629,26	336	1027,05
	24	414	654,93	405	750,91	370	894,82	379	685,86	367	875,74	432	698,84	345	870,74
	25	295	901,21	297	1053,02	329	972,59	316	849,94	296	1090,17	348	879,35	312	943,65
	26	388	726,65	431	678,12	439	701,91	524	470,38	571	463,72	446	602,52	327	1168,56
	27	374	835,20	420	784,11	392	826,67	473	645,31	509	617,35	435	689,10	244	1645,44
	28	372	854,62	412	819,06	408	760,78	447	741,57	479	648,93	407	762,04	270	1407,90
	29	383	806,77	412	753,74	380	780,92	443	754,76	397	729,32	380	862,01	303	1121,88
	30	292	1002,66	297	1027,09	321	975,12	336	958,54	295	951,63	326	1006,74	311	1112,56

Table A.15:

Total samples: 391051

channels		P3 → F3		P3 → Fz		P3 → F4		P4 → F3		P4 → Fz		P4 → F4		C3 → C4	
		n.win	avg	n.win	avg	n.win	avg	n.win	avg	n.win	avg	n.win	avg	n.win	avg
	13	367	644,48	417	447,00	275	1057,52	344	785,99	396	448,81	345	847,53	368	545,52
	14	324	801,22	440	491,45	245	1239,67	317	897,66	419	473,73	300	1033,91	364	593,84
	15	295	958,45	435	545,99	201	1565,66	280	1036,75	440	524,48	248	1276,04	368	649,52
	16	296	962,46	402	580,94	253	1207,06	312	852,65	357	658,23	305	906,71	364	672,78
	17	316	773,78	323	685,85	279	947,01	273	888,67	380	610,68	281	833,33	356	644,67
	18	245	1005,28	310	779,27	265	854,47	208	1200,95	278	871,38	242	1044,00	280	934,77
	19	201	1253,05	253	1014,35	185	1222,54	150	1635,11	259	915,55	210	1196,54	200	1368,7
	20	182	1318,0	241	1064,17	176	1424,51	165	1587,80	213	1115,78	153	1618,86	197	1341,43
freq	21	295	975,32	396	505,02	242	1248,22	305	919,26	381	528,61	269	1115,99	364	607,85
	22	247	1244,30	406	604,70	215	1441,14	261	1114,51	373	659,53	256	1180,51	388	645,29
	23	294	975,39	350	733,04	259	1151,21	255	1077,49	357	741,39	271	1014,51	379	678,01
	24	275	879,21	256	876,54	269	985,33	289	894,22	292	824,06	256	971,09	363	676,12
	25	224	1070,59	202	1134,56	180	1487,36	231	1091,46	220	1042,10	162	1712,12	250	1109,97
	26	253	1096,61	384	517,26	195	1474,53	233	1328,88	423	514,14	184	1821,51	364	606,96
	27	233	1255,21	383	566,90	158	2024,36	182	1766,92	369	661,56	198	1728,47	347	726,32
	28	258	1045,86	388	544,03	201	1584,17	229	1270,46	362	693,49	236	1253,38	334	780,58
	29	263	1008,73	357	605,11	235	1146,26	265	909,91	355	687,45	252	978,73	320	735,34
	30	200	1191,56	268	861,34	209	1275,46	220	1151,45	226	1096,45	199	1367,05	231	972,64

channels		F3 → P3		Fz → P3		F4 → P3		F3 → P4		Fz → P4		F4 → P4		C4 → C3	
		n.win	avg	n.win	avg	n.win	avg	n.win	avg	n.win	avg	n.win	avg	n.win	avg
freq	13	382	574,05	353	782,22	372	596,52	293	1024,31	276	1126,85	326	890,14	434	425,23
	14	356	681,40	338	869,20	360	681,44	271	1153,92	259	1245,45	298	999,32	468	478,57
	15	301	864,45	280	1089,49	342	829,26	283	1103,39	192	1756,67	287	1052,00	398	684,15
	16	273	908,61	261	1099,95	295	1007,92	300	947,75	221	1479,83	260	1084,48	361	769,35
	17	273	835,15	276	910,43	317	897,04	291	820,45	280	1036,08	334	718,68	320	737,05
	18	261	998,09	246	1048,19	269	911,42	284	913,05	259	985,81	229	1043,51	272	880,91
	19	223	1236,82	199	1391,28	227	1071,32	198	1405,09	206	1189,20	211	1151,89	246	1009,33
	20	191	1389,39	181	1477,40	229	1134,81	180	1584,50	174	1547,05	188	1423,47	234	1095,80
	21	324	791,30	337	782,50	351	663,73	280	1019,03	313	942,11	338	791,42	476	396,67
	22	324	822,27	320	868,97	327	793,33	286	991,0	260	1140,27	326	860,03	445	512,39
	23	312	786,39	314	841,16	313	859,56	355	713,05	277	982,24	338	735,75	430	563,18
	24	347	692,33	286	829,32	346	736,09	297	715,31	286	914,47	315	658,73	334	745,68
	25	232	1104,00	223	1119,52	281	879,97	219	1026,56	218	1169,38	255	893,50	264	968,50
	26	358	695,28	281	967,08	394	552,60	294	1004,92	264	1136,30	265	1116,70		
	27	317	938,21	306	926,38	404	629,72	245	1261,03	253	1183,36	256	1181,78	424	479,21
	28	306	934,50	331	801,61	347	747,50	243	1188,95	258	1079,62	300	915,58	401	561,69
	29	319	808,38	329	692,04	316	756,92	302	845,89	278	942,39	299	734,96	345	649,26
	30	238	1053,39	274	859,09	251	924,87	276	916,82	246	1055,21	261	813,22	274	895,90

Table A.16:

Total samples: 460171

channels		P3 → F3		P3 → Fz		P3 → F4		P4 → F3		P4 → Fz		P4 → F4		C3 → C4	
		n.win	avg	n.win	avg	n.win	avg	n.win	avg	n.win	avg	n.win	avg	n.win	avg
freq	3	405	716,89	455	404,15	446	642,57	521	434,57	462	438,90	454	643,56	419	534,75
	4	396	765,75	499	439,83	395	832,27	574	452,09	483	451,32	457	685,50	453	534,21
	5	423	757,24	515	552,28	332	1036,08	523	557,09	520	477,82	463	722,84	442	588,38
	6	459	706,27	465	677,31	335	943,85	453	615,88	500	503,43	442	693,08	431	608,15
	7	458	653,81	387	810,25	371	768,53	419	603,20	353	671,92	396	682,85	431	651,22
	8	360	851,10	563	416,26	381	727,48	434	644,58	530	398,44	402	728,10	420	611,05
	9	303	1251,40	448	752,61	290	1238,89	352	1053,80	499	606,30	320	1093,32	409	680,32
	10	259	1537,24	342	1107,35	231	1692,29	286	1362,71	442	795,98	334	1118,90	375	842,23
	11	312	1088,66	325	1034,38	281	1268,72	285	1173,17	349	946,42	343	946,21	361	882,78
	12	214	1711,75	239	1315,50	185	2008,50	215	1689,39	295	1170,63	208	1712,27	250	1270,87

channels		F3 → P3		Fz → P3		F4 → P3		F3 → P4		Fz → P4		F4 → P4		C4 → C3	
		n.win	avg	n.win	avg	n.win	avg	n.win	avg	n.win	avg	n.win	avg	n.win	avg
freq	3	409	670,76	472	561,36	445	446,09	428	353,44	494	402,24	532	332,54	416	631,63
	4	447	621,62	444	619,30	466	506,57	464	388,10	520	460,10	553	421,34	412	687,99
	5	440	626,41	436	654,30	444	607,34	468	463,76	480	590,14	484	561,38	423	702,84
	6	458	555,89	419	652,61	435	607,45	449	549,20	457	622,59	387	684,76	455	608,05
	7	417	590,89	410	687,99	407	638,38	394	664,12	326	856,85	375	717,51	387	727,07
	8	469	465,41	498	434,95	498	446,71	542	376,87	473	371,53	553	356,56	455	598,86
	9	513	524,84	564	505,75	563	499,48	572	479,87	527	468,75	528	508,93	419	806,65
	10	483	646,23	489	648,78	474	692,63	490	641,32	468	665,08	404	752,31	388	953,51
	11	393	680,74	362	648,49	420	669,67	434	654,32	454	625,25	340	850,55	378	830,11
	12	302	1076,67	325	895,50	292	1025,77	326	747,07	316	946,229	290	1071,64	283	1177,96